- Master Thesis in Climate Dynamics -

Winter circulation anomalies in 2009/10 & 2013/14, and associated forcing mechanisms

Helene Asbjørnsen

June 2016

Geophysical Institute
University of Bergen

Acknowledgements

First and foremost I would like to thank my supervisors Camille Li and Stefan Sobolowski for providing such an interesting research opportunity for my thesis work. Thank you for being engaging, motivating and patient. Your feedback has been invaluable during this process, and I am truly grateful for all your help. I would also like to thank family and friends for your support and encouragement during this time. Finally, a special thanks to my fellow students for five memorable years filled with laughs, long coffee breaks, and a little bit of studies in between. Thanks for brightening up any ordinary day.

Abstract

Recent cases of severe winter weather in midlatitude regions have been linked to large-scale atmospheric circulation anomalies, but the physical mechanisms driving such anomalies are poorly understood. In this study the circulation anomalies of two recent winters, 2009/10 and 2013/14, are investigated using a linear stationary wave model. As the model reproduces the observed atmospheric circulation of the two winters, it can be used to isolate and determine the effects of orographic features, diabatic heating patterns, transient eddies, and nonlinear interactions in forcing the anomalous circulation patterns. The results show that none of these forcing factors alone are responsible for the circulation anomalies seen in 2009/10 and 2013/14. Still, large parts of the anomaly fields are forced by diabatic heating, in combination with stationary nonlinear effects in 2009/10, and transient forcing in 2013/14. The diabatic heating response is thought to mainly originate from strong warm SST anomalies in the central tropical Pacific associated with an El Niño event in 2009/10, and moderate warm SST anomalies in the western tropical Pacific associated with a positive phase of the North Pacific mode in 2013/14. The different SST patterns generate slightly different circulation anomaly patterns the two winters. Eddy-mean flow interactions, and other processes where nonlinearity is important, contribute to enhance these differences, resulting in the contrasting circulation anomalies observed in 2009/10 compared to 2013/14.

Contents

List of Figures

Abbreviations

SST	**S**ea **S**urface **T**emperature
NAO	**N**orth **A**tlantic **O**scillation
SW	**S**tationary **W**ave
AO	**A**rctic **O**scillation
GCM	**G**eneral **C**irculation **M**odel
SWM	**S**tationary **W**ave **M**odel
EOF	**E**mpirical **O**rthogonal **F**unction

Chapter 1

Introduction

1.1 Problem statement

The record-breaking winter weather of 2009/10 and 2013/14 was associated with large-scale atmospheric circulation anomalies in the midlatitudes, but the physical mechanisms behind such winter anomalies are poorly understood. The 2009/10 and 2013/14 winter seasons were especially remarkable for the persistent cold spells in eastern North America, and for 2009/10 also in northern Europe. A series of recent cold, snowy winters in midlatitude regions, such as those seen in 2009/10 and 2013/14, has initiated a debate among climate scientists regarding the underlying causes of such winter anomalies. Are the observed circulation anomalies related to natural variability within the climate system or can these anomalies be indicative of more systematic changes in our climate system related to global warming?

In this study the forcing mechanisms behind the altered circulation patterns in 2009/10 and 2013/14 are explored using an idealized dynamical model. This approach poses the problem within a simplified framework, allowing us to isolate the effects of various forcings and study them in detail, assuming a set of simplifying assumptions is valid. Our focus will be Northern Hemisphere winter circulation anomalies in midlatitude regions, and the associated forcing mechanisms.

1.2 Background

Global temperatures have risen over the past century due to a human induced increase in greenhouse gases (Hartmann et al., 2013). As of 2016, global mean temperatures have increased by approximately 1°C since pre-industrial times. Over the past 50 years global temperatures have been increasing at a rate nearly double that of the last 100 years, indicating an accelerating warming as seen in Figure 1.1. Most pronounced is the warming in the Arctic region, which is warming at a rate nearly double that of lower latitudes. This phenomenon is known as Arctic amplification. Arctic amplification is characterized by intensified near-surface warming in winter, with temperature feedbacks and the snow-ice-albedo feedback identified as two of the main drivers (Pithan and Mauritsen, 2014). We know that the global warming and Arctic amplification signals have the potential to affect large-scale circulation patterns, but to what extent is still uncertain (Shepherd, 2014; Trenberth et al., 2015). It remains particularly unclear whether or not global warming plays a role in producing anomalous seasonal patterns such as those associated with the winters of 2009/10 and 2013/14.

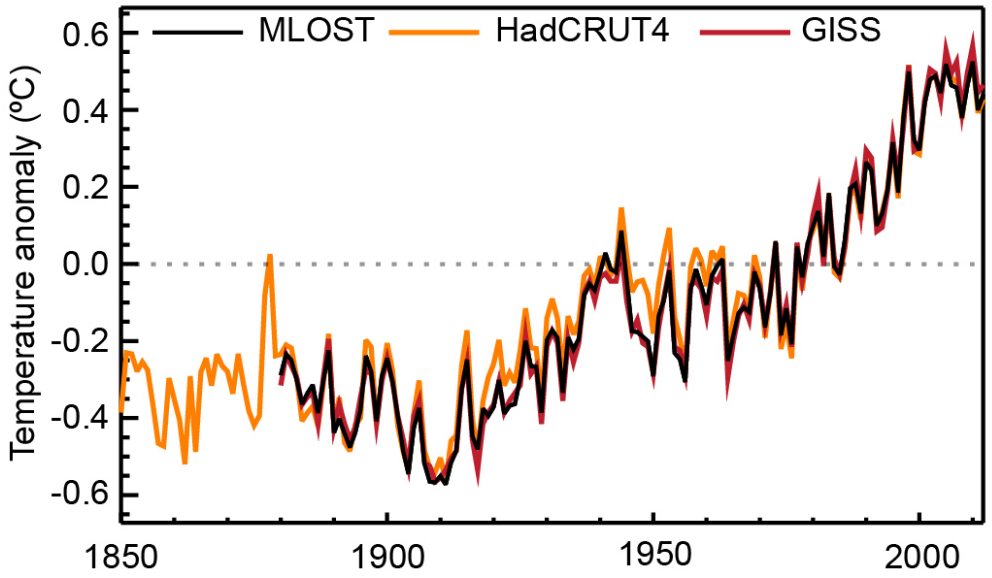

FIGURE 1.1: Annual global mean surface temperature anomalies relative to a 1961-1990 climatology from three combined land-surface air temperature and sea surface temperature data sets (HadCRUT3, GISS and NCDC MLOST) (Hartmann et al., 2013).

The anomalous winter weather of 2009/10 was characterized by persistent cold spells in eastern North America and northern Europe, while 2013/14 was mild and stormy in western Europe, cold and snowy in eastern North America, and

warm and dry in western North America. Although both winter seasons had noticable cold anomalies in midlatitude regions, 2009/10 and 2013/14 can be regarded as contrasting in other ways. In 2009/10, the NAO was in a strong negative phase, reflected by a zonally oriented and equatorward shifted Atlantic jet (Figure 1.2e). The negative NAO was accompanied by extensive cold anomalies in northern Europe and parts of eastern North America, while the Canada and Greenland regions were anomalously warm (Figure 1.2c). A strong El Niño event, with warm SST anomalies in the central tropical Pacific, was present this year, while cold SST anomalies were present in the northeastern Pacific (Figure 1.2a). A strong El Niño signal is also apparent in the diabatic heating anomaly field of 2009/10 (Figure 1.3a), and the Pacific jet is visibly extended eastward (Figure 1.2e), which is typical for a central Pacific El Niño winter (Graf and Zanchettin, 2012). In 2013/14, the NAO was in a positive phase, reflected by a slightly southwest-northeast tilted and poleward shifted Atlantic jet (Figure 1.2f), though not as pronounced as for a canonical positive NAO. Western Europe experienced a relatively mild winter this year, with storms repeatedly hitting the UK and the coast of France. Strong winds and heavy rainfall led to extensive flooding, and the 2013/14 winter ended up being the UK's wettest winter on record (Kendon and McCarthy, 2015). An unusual flow pattern over North America, reflected by a poleward deflection and weakening of the Pacific jet exit (Figure 1.2f), led to record-breaking cold temperature and snowfall events for numerous metropolitan areas in eastern North America, and a dry, warm winter, with drought conditions in California, in western North America (Wang et al., 2014). Remarkably strong warm SST anomalies in the North Pacific and moderate warm SST anomalies in the western tropical Pacific warm pool region were present this year (Figure 1.2b), while a strong heating anomaly in the western tropical Pacific is apparent in the diabatic heating anomaly field (Figure 1.3b).

The differences in weather conditions between these two winters are linked to differences in atmospheric circulation, which are clearly seen in the observed stationary wave patterns (Figure 1.2g,h). The stationary wave pattern shows the deviation from zonal symmetry of the time-averaged large-scale flow. This deviation is generated by asymmetries at the Earth's surface, such as land-ocean temperature contrasts and orography, as well as zonally asymmetric effects from heating and transient eddies within the atmosphere. Looking at the upper-level

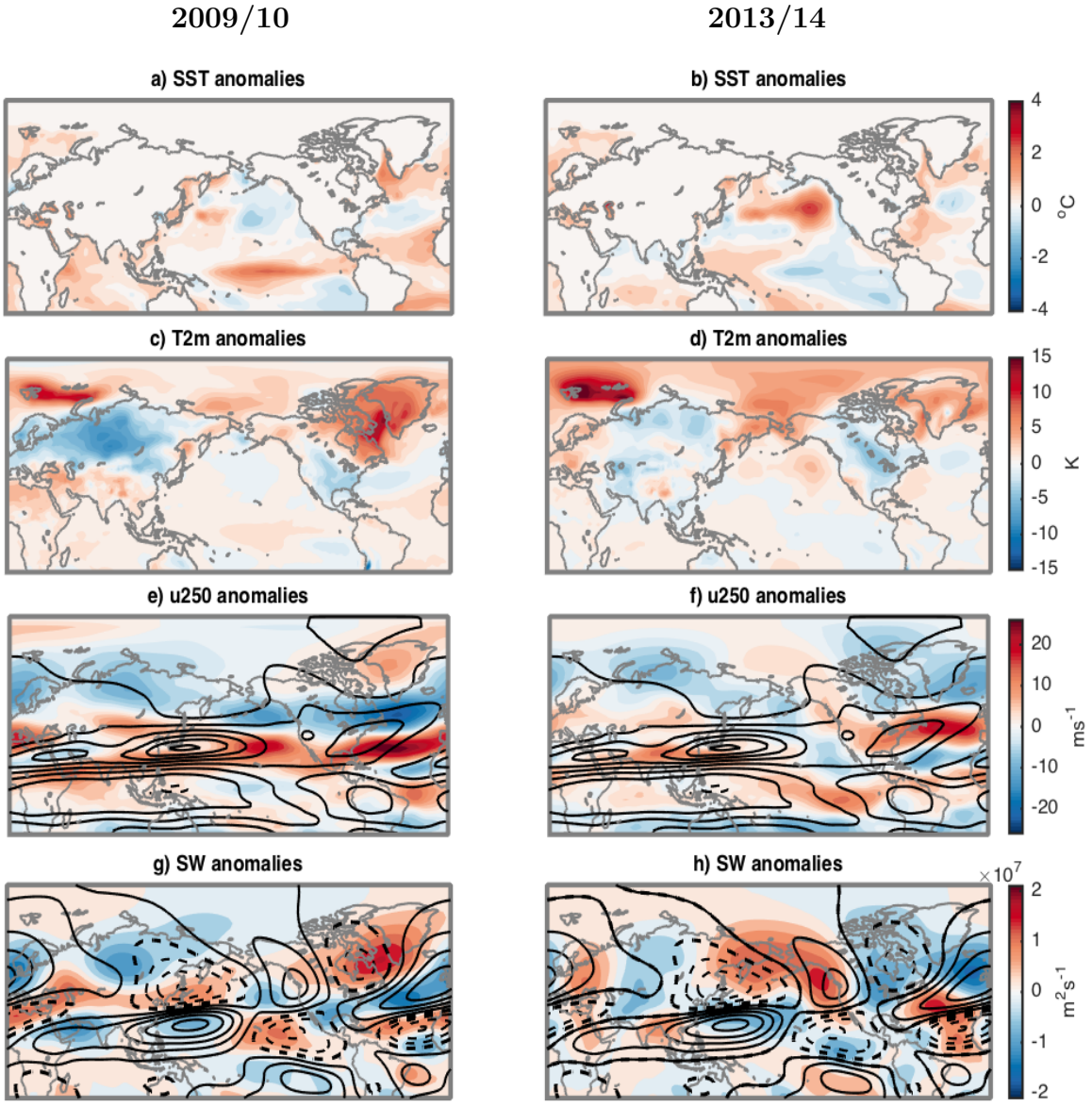

FIGURE 1.2: (a)-(b): Winter (DJF) SST anomalies relative to climatology ($2° \times 2°$ gridded data from http://www.esrl.noaa.gov/psd/data/gridded/data.noaa.ersst.html). (c)-(d): Winter (DJF) 2m temperature anomaly relative to climatology (NCEP-NCAR reanalysis). (e)-(f): Winter (DJF) upper-level (250hPa) zonal wind anomaly (shadings) relative to climatology (10 ms^{-1} contours) (NCEP-NCAR reanalysis). (g)-(h): Winter (DJF) upper-level (sigma=0.2582) stationary wave anomalies (shadings) relative to climatology (6×10^6 m^2s^{-1} contours) in asymmetric streamfunction (NCEP-NCAR reanalysis). (a)-(h): 1981-2000 as climatological period.

tropospheric stationary wave pattern is useful when studying jet variability, as it indicates the position and the meandering of the jet. The positioning of the jets is important for determining the paths synoptic systems take, and consequently the overall character of midlatitude storm tracks and weather patterns. Additionally, the magnitude of the stationary wave pattern is indicative of planetary wave amplitudes, which are closely associated with temperature extremes in midlatitude regions (Screen and Simmonds, 2014). In this study, upper-level stationary waves

will be used as an indicator of the time-averaged winter circulation.

The winter stationary wave patterns of 2009/10 and 2013/14 were in many ways contrasting. The climatological winter stationary wave pattern (contour lines in Figure 1.2g,h), where positive (negative) streamfunction denotes a ridge (trough) or anticyclonic (cyclonic) circulation, is characterized by a quadrapole pattern of ridges and troughs over the Pacific Ocean and a dipole pattern of a ridge and a trough over the Atlantic Ocean. The climatological ridge over western North America and the climatological trough over eastern North America (from here on referred to as the North American ridge-trough pattern) are of special interest to us as they are indicative of the flow pattern over North America. In 2009/10, an overall weakening of the climatological North American ridge-trough pattern is seen in Figure 1.2g (negative anomaly over ridge and positive anomaly over trough). This is consistent with a more zonal large-scale flow, as seen in Figure 1.2e. In 2013/14, a strengthening of this climatological stationary wave over North America is seen in Figure 1.2h (positive anomaly over ridge and negative anomaly over trough), with a more enhanced ridge-trough pattern. This was associated with a more meandering jet. The stationary wave pattern over the Atlantic region is also interesting, as it closely relates to the Atlantic jet and the weather conditions in western Europe. In 2009/10, the climatological Atlantic ridge is clearly weakened (Figure 1.2g), and this is consistent with a zonalized Atlantic jet. In 2013/14, there is a southwest strengthening and northeast weakening of the climatological Atlantic ridge center (Figure 1.2h), indicating a tilted Atlantic jet. A detailed description of the climatological stationary wave pattern will be given in section 2.2.1, while the 2009/10 and 2013/14 stationary wave anomaly fields will be discussed further in section 3.1 and 3.2.

Various forcing mechanisms have been proposed to explain the 2009/10 and 2013/14 circulation anomalies, but there is still no consensus on which mechanisms were the dominant ones. The midlatitude circulation anomalies that we are interested in can be forced by local anomalies, such as local SST variability, and/or remotely by tropical or Arctic anomalies, such as tropical SST variability and changes in Arctic sea ice extent. These anomalies are either connected to natural variability within the climate system or to systematic changes in the climate system related to external forcings such as global warming. In a complex climate system there is

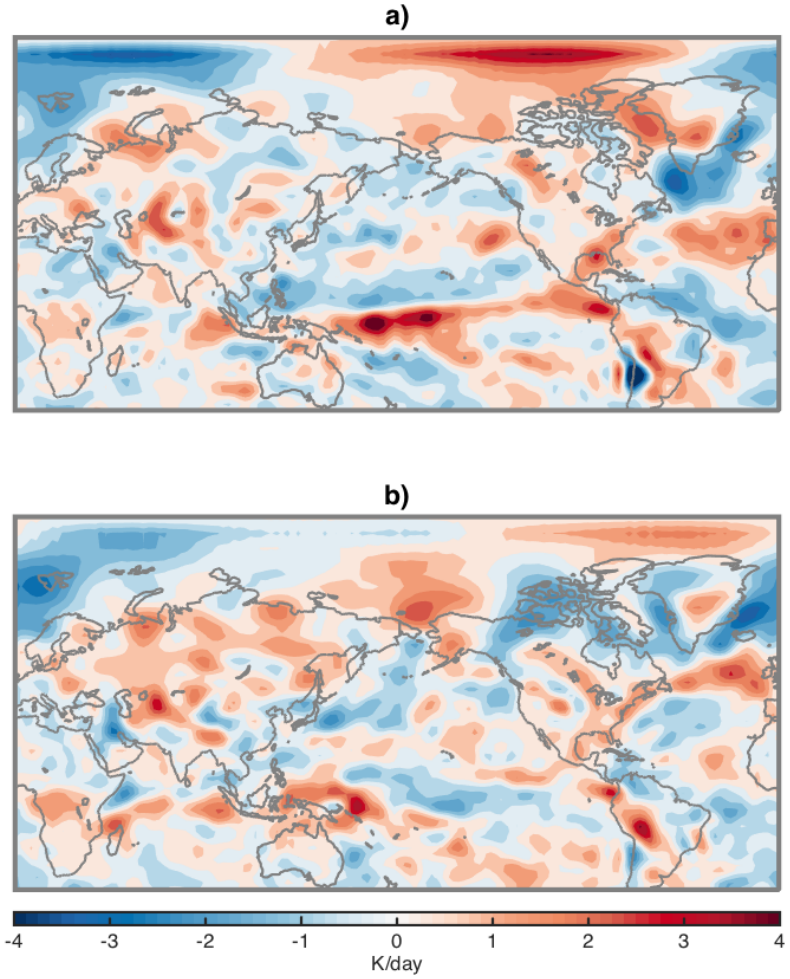

FIGURE 1.3: Winter (DJF) column-averaged mass-weighted diabatic heating anomaly of (a) 2009/10 and (b) 2013/14 relative to climatology (1981-2000).

no simple relationship between cause and effect, and the different forcing mechanisms proposed are not necessarily mutually exclusive. The next two paragraphs will summarize some of the prominent hypotheses addressing recent winter circulation anomalies, and the forcing mechanisms proposed to be the main driver of them.

Some studies suggest that the circulation anomalies observed in 2009/10 and 2013/14 are related to natural variability within the climate system. The cold, snowy winter of 2009/10 has been linked to the low temperatures accompanying a strong negative NAO combined with an El Niño event (Seager et al., 2010). The winter of 2013/14 has been linked to warm SST anomalies in the North Pacific associated with an extreme positive phase of the North Pacific mode since mid 2013 (Hartmann, 2015; Wang et al., 2014). The North Pacific mode is a variability pattern in Pacific SSTs where, when in a positive phase, warm SST anomalies

are typically present in the western tropical Pacific and extending northeast along the California coast. This type of SST pattern is visible in Figure 1.2b, and has been shown to drive downstream flow anomalies that results in an enhanced ridge-trough pattern over North America, as seen in 2013/14 (Hartmann, 2015). The observed SST anomalies in the North Pacific this winter have been linked to warm SSTs in the western tropical Pacific, which is a region early on identified as an optimal location for SST anomalies to force midlatitude circulation anomalies (Palmer and Mansfield, 1984). For both 2009/10 and 2013/14, Riviére and Drouard (2015) suggest synoptic wave breaking over North America as a possible pathway communicating large-scale flow anomalies in the North Pacific to the North Atlantic sector. Specifically, Riviére and Drouard (2015) argue that the 2009/10 and 2013/14 flow conditions in the North Pacific were responsible for shaping synoptic wave-trains favoring cyclonic/anticyclonic wave breaking, which influenced the NAO by shifting the Atlantic jet equatorward/poleward, and thus affecting the winter weather in the Atlantic region.

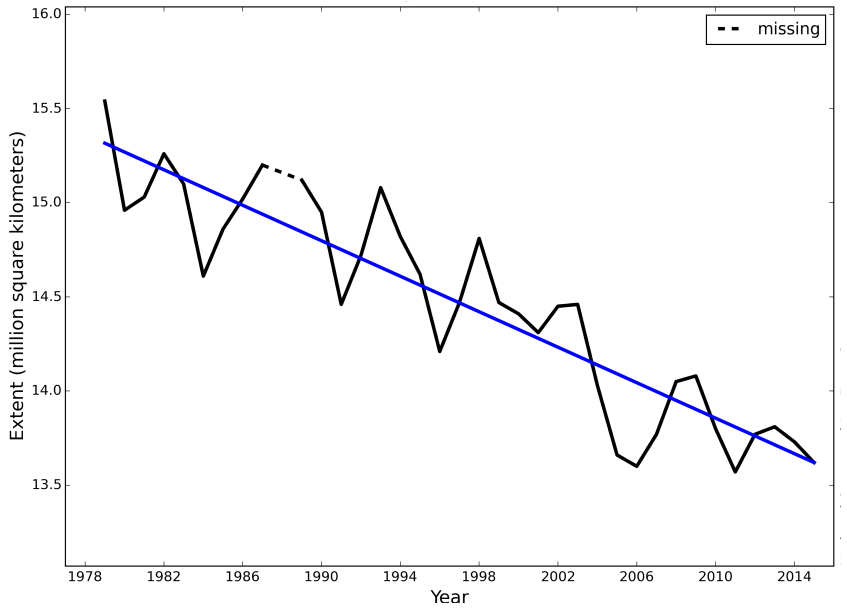

FIGURE 1.4: Average monthly January Arctic sea ice extent from 1979 to 2015 from the National Snow and Ice Data Center (retrieved at http://nsidc.org/arcticseaicenews/2015/02/vary-january/).

Other studies suggest that the recent midlatitude circulation anomalies are due to forcing mechanisms related to Arctic sea ice reductions, but there is still little robust evidence supporting this hypothesis. Possible dynamical pathways suggested for the Arctic to drive midlatitude circulation anomalies can be divided into three groups: 1) changes in the storm tracks directly due to variability in sea

ice and snow cover, 2) changes in the jet stream due to reduced equator-to-pole temperature gradient, and 3) vertical propagation of planetary waves weakening the stratospheric polar vortex and consequently shifting the NAO/AO towards negative phase (Cohen et al., 2014). The equator-to-pole gradient hypothesis has been particularly prominent in the literature as well as in the media. Francis and Vavrus (2012) argue that the equator-to-pole temperature gradient is reduced due to amplified warming of the Arctic, compared to the lower latitudes. This leads to weakened westerly winds, through the thermal wind relation, and increased planetary wave amplitudes, which in turn causes weather patterns to propagate eastward more slowly. These conditions are favorable for blocking events, known to be associated with weather extremes such as cold spells and heat waves. The limited evidence from observational studies supporting this hypothesis is pointed out in several papers (Barnes, 2013; Barnes et al., 2014; Screen and Simmonds, 2013), and the theoretical arguments alone are not sufficiently sound (Wallace et al., 2014). If applying the equator-to-pole gradient hypothesis to our two winters of interest, it is clear that only 2013/14 fits the hypothesis with an amplified planetary wave pattern, even though the sea ice extent in early winter (Nov-Dec) was similar and below normal both seasons, while for instance the 2014 January sea ice extent was only slightly lower than that of 2010 (Figure 1.4). This indicates that even if a casual link between midlatitude circulation and sea-ice loss might exist, the relationship is complex and the influence of natural variability is substantial.

1.3 Research questions

This study will investigate some of the proposed forcing mechanisms of the 2009/10 and 2013/14 anomalous stationary wave patterns, and our goal is to identify the main forcing factors and their relative importance. For instance we know that both Pacific SST anomalies and reduced Arctic sea ice extent will affect the diabatic heating field, and could therefore possibly alter the stationary wave pattern in 2009/10 and 2013/14. Global warming has modified the atmospheric background state on which planetary waves propagate, and this could impact the stationary wave pattern. Interaction between the mean flow and transient eddies could also be an important factor, especially for the Atlantic response, as indicated by Riviére

and Drouard (2015). With this study we seek to answer the following questions: Which forcing factors contribute the most to the anomalous circulation patterns in 2009/10 and 2013/14? Can these winters be explained completely, or in part, by a single forcing factor, or is it a combination? Are the main contributing forcings the same for 2009/10 and 2013/14 in areas where the impacts are similar? If not, what could explain this? What is the potential role of climate change these winters?

Chapter 2

Methods

In order to improve our understanding of large-scale winter circulation anomalies it is necessary to identify the main forcing factors contributing to these anomalies, and their relative importance. A case study approach focusing on the 2009/10 and 2013/14 Northern Hemisphere winter seasons provides an opportunity for an in-depth study of observed circulation anomalies. In a complex climate system, with natural variability and chaotic processes operating on all time scales in addition to external forcing such as global warming, there is no simple relationship between cause and effect. Here, we analyze two recent winter seasons using an idealized dynamical model; a tool that includes many simplifying assumptions about the climate system, but that allows us to make inferences about the cause of the observed large-scale circulation anomalies of 2009/10 and 2013/14. A complete description of the model used can be found in the appendices of Ting and Held (1990) and Ting (1994); a more basic description is provided in section 2.1, along with a brief evaluation of its performance in section 2.2.

2.1 Stationary wave model

The linear stationary wave model used provides an idealized framework for exploring the contributions of specific forcing factors to the 2009/10 and 2013/14 winter circulation anomalies. The model is a baroclinic, steady state model based on the dynamical core of NOAA's Geophysical Fluid Dynamics Laboratory's Global

Dynamics Group spectral GCM (Ting, 1994). A comprehensive GCM incorporates complicated physical atmospheric and surface processes, and interactions between these processes, that are highly idealized in the stationary wave model used. However, unlike a comprehensive GCM, the stationary wave model allows us to separate the effect of the individual forcings of stationary waves by simple exclusion/inclusion of the forcing terms. Given that the assumption of linearity is valid, causality can be implied, meaning that we can determine which forcing factors create the circulation anomalies of interest. This makes the model a useful tool in interpreting GCM output and observational data. It is well documented that the model reproduces observed climatological stationary wave patterns (Held et al., 2002; Ting, 1994, 1996; Ting and Held, 1990; Wang and Ting, 1999). Upper-level tropospheric winter stationary waves, which are the focus of this study, are simulated especially well according to Wang and Ting (1999).

The stationary wave model is linearized about a zonally symmetric basic state and is driven by four asymmetric forcings: orography, diabatic heating, transient forcing and stationary nonlinearity. All forcings are calculated from daily NCEP-NCAR reanalysis data on a $2.5^\circ \times 2.5^\circ$ global grid with 17 verical levels (Kalnay et al., 1996). Before calculating the forcing terms, the reanalysis data is interpolated onto the model grid, which is a R30 (rhomboidal wavenumber 30 truncation) grid with 2.25° latitude $\times$ 3.75° longitude resolution, and 14 unevenly spaced sigma levels in the vertical. The basic state represents a mean state of the atmosphere for each calendar month of the year, and includes the following variables: zonal wind, meridional wind, temperature, surface pressure and sigma dot vertical velocity. These monthly means can be calculated for specific multi-year periods or for individual years.

The four forcing terms provide the zonal asymmetries that create the stationary waves:

1) The orographic forcing is a mechanical forcing, and represents the forcing exerted on the large-scale flow by mountains and terrain at the Earth's surface (Hoskins and Karoly, 1981). The orography itself is time-invariant, but the effect of the orographic forcing is not constant because it depends on the background flow (i.e., the basic state about which the model is linearized).

2) Diabatic heating is a thermal forcing usually calculated as a residual from the thermodynamic equation, as it is difficult and costly to measure directly (Chan and Nigam, 2009). The diabatic heating term includes heating sources and sinks, such as radiative, sensible and latent heat fluxes, that contribute to changing the temperature of the air column. In this study, also the transient heat flux is included in the diabatic heating term. A limitation to calculating the diabatic heating as a residual is not being able to distinguish between the different processes that create the observed diabatic heating anomalies of interest. In Northern Hemisphere winter, the diabatic heating field typically shows cooling over Eurasia and North America with heating centers over the North Pacific and North Atlantic oceans (Figure 2.1), as the winter atmosphere generally loses heat over continental areas and gains heat over oceanic areas (Wang and Ting, 1999).

3) The transient forcing accounts for the effect of storm activity, and other high frequency perturbations of the mean flow, through eddy fluxes of vorticity and divergence.

4) The forcings discussed above are not independent of each other, but interact through nonlinear interactions (Held et al., 2002). However, linear models do not account for such interactions, and as a result a final forcing term is needed; the stationary nonlinear forcing. The stationary nonlinear forcing accounts for all nonlinear interactions between the background flow (basic state) and the asymmetric forcings, as well as interactions between the different asymmetric forcings. A limitation to using a linear stationary wave model is not being able to separate between different nonlinear interactions and their relative contributions to the stationary wave field. For this, a nonlinear version of the model has to be used.

In addition to the forcing terms, three damping terms are present in the model: Rayleigh friction, Newtonian cooling and biharmonic diffusion. Rayleigh friction represents the drag exerted on the flow by the lower boundary. Newtonian cooling is applied as a thermal damping term that represents heat transfer with the surface. Biharmonic diffusion is implemented to remove small-scale noise.

The stationary wave model produces monthly steady-state solutions in the following manner. First, the model equations are time-averaged over a month so

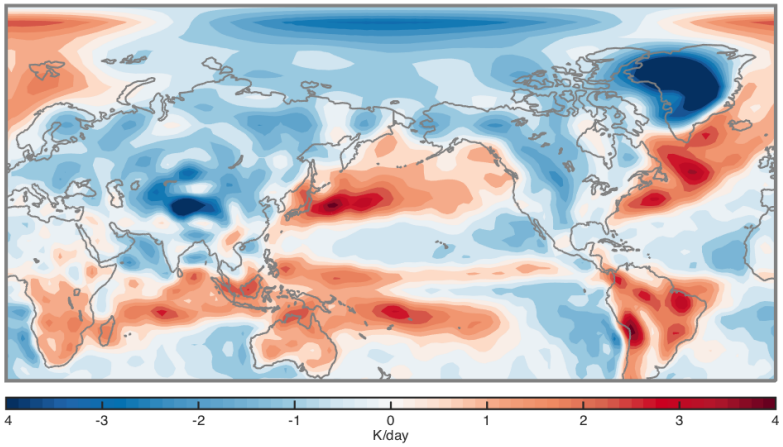

FIGURE 2.1: Climatological (1981-2000) winter (DJF) column-averaged mass-weighted diabatic heating field.

that the time tendency terms ($\frac{\partial}{\partial t}$) in the prognostic equations can be neglected, leaving us with a steady-state problem. These model equations are the prognostic equations for vorticity, divergence, temperature, and surface pressure. Additionally the hydrostatic and mass continuity equations are needed to determine the geopotential height and the sigma dot vertical velocity. Second, the time-averaged model equations are linearized about the zonal mean basic state, and the zonally symmetric terms are removed, leaving only the asymmetric terms generating stationary waves. In these equations there are four types of forcings present. Orography enters through the hydrostatic equation as the lower boundary condition. Diabatic heating enters directly through the thermodynamic equation (transient heat flux included). The transient forcing enters through the vorticity and divergence equations as long-term means of eddy vorticity and divergence fluxes. The nonlinear terms discarded in the linearization are treated as a separate forcing term of stationary nonlinear heat, vorticity and divergence fluxes, and is referred to as the stationary nonlinear forcing. Finally, the model separates the model equations into zonal wave numbers *m=1,2,3... 30*, and sets up a matrix equation of the form $A_m X_m = B_m$, where B is the forcing matrix, A contains the information of the basic state, and X is the unknown stationary wave solution. This equation is solved by matrix inversion for each wavenumber m. The entire process is repeated for each month of the year, leaving us with monthly stationary wave solutions. For more details on the model equations the reader is directed to the appendix of Ting (1994), and for a thorough description of the matrix inversion method the reader is directed to the appendix of Ting and Held (1990).

Throughout the thesis we concentrate on the stationary wave solutions for the December to February winter season (DJF) at upper tropospheric level (sigma level 0.257 or approximately 250hPa).

2.2 Simulations

A series of simulations was carried out to test how well the model performs in general (section 2.2.1), before concentrating on forcing experiments designed to determine the relative contributions of the four asymmetric forcings to the 2009/10 and 2013/14 stationary wave anomalies (section 2.2.2).

2.2.1 Control run

A control simulation was first performed in order to see how well the model performs for a climatological period. For this simulation, the stationary wave model was run with all four forcing terms and basic state calculated for the climatological period 1981-2000. This will be our climatological control period throughout the thesis. The stationary wave pattern generated is shown in Figure 2.2f. When comparing the full stationary wave field produced by the model (Figure 2.2f) to reanalysis (Figure 2.2h), it is clear that the model performs well for this control period. The positioning of the Pacific quadrapole pattern and the Atlantic dipole pattern is consistent with reanalysis. These are major features of ridges and troughs located over the ocean basins, characteristic for the winter stationary wave pattern. In the Atlantic region the stationary wave magnitude and shape are captured particularly well by the model. The shape of the North American ridge is also well reproduced, with a characteristic nortwestward tilt over Alaska. Even though the model overall performs satisfactorily for the control period, there are some discrepancies that must be mentioned. These discrepancies are generally consistent with those found in Wang and Ting (1999) (Figure 2.3). 1) The model shows signs of exaggerating the stationary wave magnitudes compared to reanalysis in the Pacific region. This is especially true for the North American ridge centered over the U.S. west coast, which is simulated to have higher magnitudes than what is observed in the reanalysis data. 2) There are some discrepancies in

the high-latitude regions. This is expected to a certain degree because the assumption of scale separation of the waves breaks down at higher latitudes. Especially noticeable is the North American trough, which is centered over the Hudson Bay region in reanalysis, but extends northwest and stretches into the Arctic Ocean in the model simulation. As opposed to what was found in Wang and Ting (1999) (Figure 2.3), this trough is sligthly weaker in the model simulation compared to reanalysis.

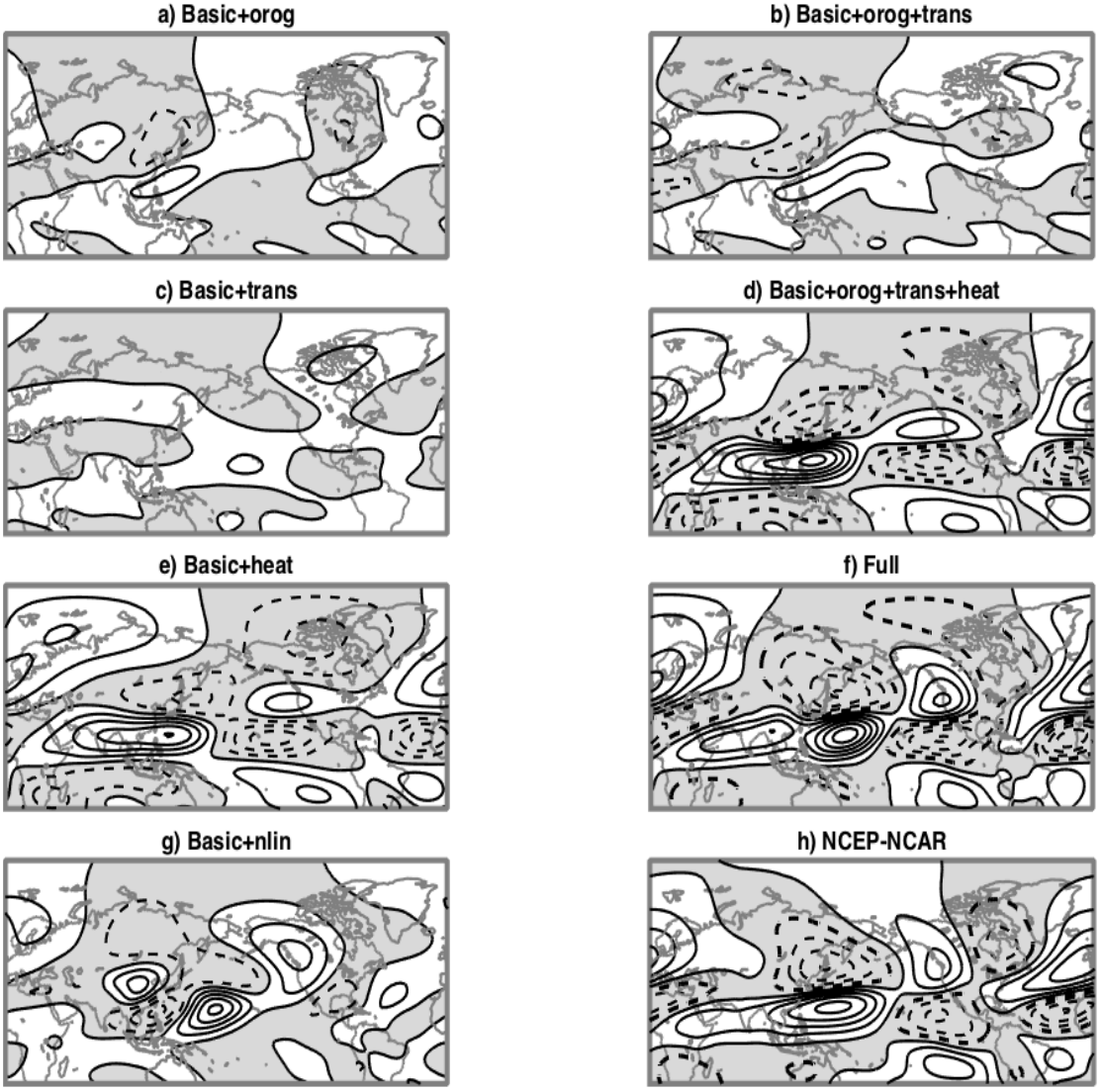

FIGURE 2.2: (a)-(g): Decomposition of the winter (DJF) upper-level ($\sigma = 0.257$) stationary wave field for the climatological control period (1981-2000) in asymmetric streamfunction (6×10^6 $m^2 s^{-1}$ contours), from SWM. (h): Winter (DJF) upper-level (250hPa) stationary wave field for the climatological control period (1981-2000) in asymmetric streamfunction (6×10^6 $m^2 s^{-1}$ contours), from NCEP-NCAR reanalysis. (a)-(h): Solid contours indicate positive streamfunction, dashed contours and grey shaded areas indicate negative streamfunction.

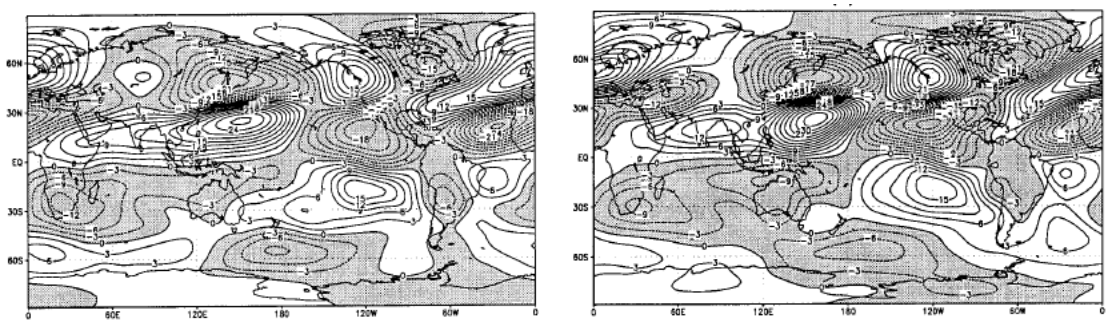

FIGURE 2.3: Winter (Jan) upper-level ($\sigma = 0.257$) stationary wave field for the climatological period 1985-1993 in asymmetric streamfunction ($3 \times 10^6\ m^2 s^{-1}$ contours), from NCEP-NCAR reanalysis (left), and from SWM (right) (Wang and Ting, 1999).

To further explore how the individual forcing terms contribute to the full winter stationary wave pattern, the model was run with the forcings applied one at the time. This was done by excluding/including the different forcing terms when running the model, still linearized about the control period basic state. The stationary wave patterns generated when running the model with the four asymmetric forcings separately (Figure 2.2a,c,e,g) add linearly to the full field seen in Figure 2.2f.

1) The orographic forcing generates wavetrains downstream of major orographic features; specifically the Tibetan Plateau and the Rocky Mountains in the Northern Hemisphere (Figure 2.2a). The meridional extent and height of the Tibetan Plateau typically causes it to force more pronounced stationary waves than the Rockies (Held et al., 2002), something which is consistent with what is seen in Figure 2.2a.

2) Diabatic heating is clearly the most dominant forcing of winter stationary waves in the climatological control period used (Figure 2.2e). However, studies show that the relative importance of diabatic heating compared to orography in forcing stationary waves is quite sensitive to the atmospheric background flow (basic state), and especially the zonal mean low-level wind strength (Chen, 2001; Held and Ting, 1990). Major features of the full winter stationary wave pattern seen in Figure 2.2f, such as the Pacific quadrapole and the Atlantic dipole, are generated by the diabatic heating term alone. The ocean-land thermal contrasts seen in Figure 2.1 cause these features to be centered over the edges of the ocean basins. In winter season these contrasts are particularly large compared to summer, making the winter

stationary wave pattern more pronounced (Wang and Ting, 1999). Because the Northern Hemisphere has a larger fraction covered by landmasses than the Southern Hemisphere, the combined effect of orographic features and ocean-land thermal contrasts leaves the northern hemispheric stationary waves more pronounced. The diabatic heating forcing appears to be causing the previously mentioned overly stretched out North American trough in the full field compared to reanalysis. Inaccuracies in the derived diabatic heating field could possibly explain this discrepancy.

3) The transient forcing is a relatively weak contributor to the full stationary wave field. Transient eddy forcing is often referred to as a destructive forcing, as it generally contributes to dampen the overall stationary wave pattern generated by the other forcings (Held et al., 2002; Wang and Ting, 1999). This is consistent with what is seen in Figure 2.2c, where the transient eddies contribute to slightly dampen the North American ridge-trough pattern and the Atlantic ridge.

4) The stationary nonlinear forcing contributes to shifting the stationary wave pattern eastward, something which is apparent when comparing Figure 2.2d to Figure 2.2f. The stationary nonlinearity is also important for maintaining the North American ridge; specifically it strengthens and elongates the ridge northwestward (Figure 2.2g). It is well documented that this strengthening of the North American ridge is due to nonlinear interactions by the Rocky Mountains, and studies show that interactions between flows forced by diabatic heating and orography are particularly important to this effect (Ringler and Cook, 1999; Ting et al., 2001). Although the stationary nonlinear term is necessary for the model to capture the shape of the North American ridge seen in reanalysis, it also appears to be causing the exaggerated ridge magnitude in the model simulation compared to reanalysis.

2.2.2 Forcing experiments

For the 2009/10 and 2013/14 winter seasons, a set of experiments was carried out where the stationary wave response to different combinations of the four asymmetric forcings was explored.

	Basic state	Orography	Transient forcing	Diabatic heating	Stationary nonlinearity
Full	✓	✓	✓	✓	✓
Basic+orog	✓	✓	-	-	-
Basic+trans	✓	-	✓	-	-
Basic+heat	✓	-	-	✓	-
Basic+nlin	✓	-	-	-	✓
Basic+orog+trans	✓	✓	✓	-	-
Basic+orog+heat	✓	✓	-	✓	-
Basic+orog+nlin	✓	✓	-	-	✓
Basic+trans+heat	✓	-	✓	✓	-
Basic+trans+nlin	✓	-	✓	-	✓
Basic+heat+nlin	✓	-	-	✓	✓
Basic+orog+trans+heat	✓	✓	✓	✓	-
Basic+orog+trans+nlin	✓	✓	✓	-	✓
Basic+orog+heat+nlin	✓	✓	-	✓	✓
Basic+trans+heat+nlin	✓	-	✓	✓	✓

TABLE 2.1: Table of forcing combinations and corresponding experiment name. The sign (✓) idicates that the forcing is included in the SWM run and set to 2009/10, 2013/14 or climatology, while the sign (-) indicates that the forcing is excluded.

The stationary wave model was run with the basic state of choice and the corresponding asymmetric forcings excluded/included as indicated in Table 2.1. The name of a particular forcing experiment indicates the forcings included in the run; forcings not present in the experiment name are set to zero. The fifteen different forcing experiments account for all possible combinations of the four asymmetric forcings. This same set of experiments was repeated with the monthly 2009, 2010, 2013, 2014, and climatological control period basic state and forcings. From the monthly stationary wave output of these runs, the seasonal averages were computed to obtain the December 2009 to February 2010 (DJF 2009/10), December 2013 to February 2014 (DJF 2013/14), and December to February climatological stationary wave patterns (DJF 1981-2000).

In order to obtain the modeled response to a particular forcing or forcing combination in 2009/10 (2013/14), the climatological control run corresponding to that particular forcing experiment is subtracted. This leaves us with the isolated response to the forcing or forcing combination for the winter season of interest.

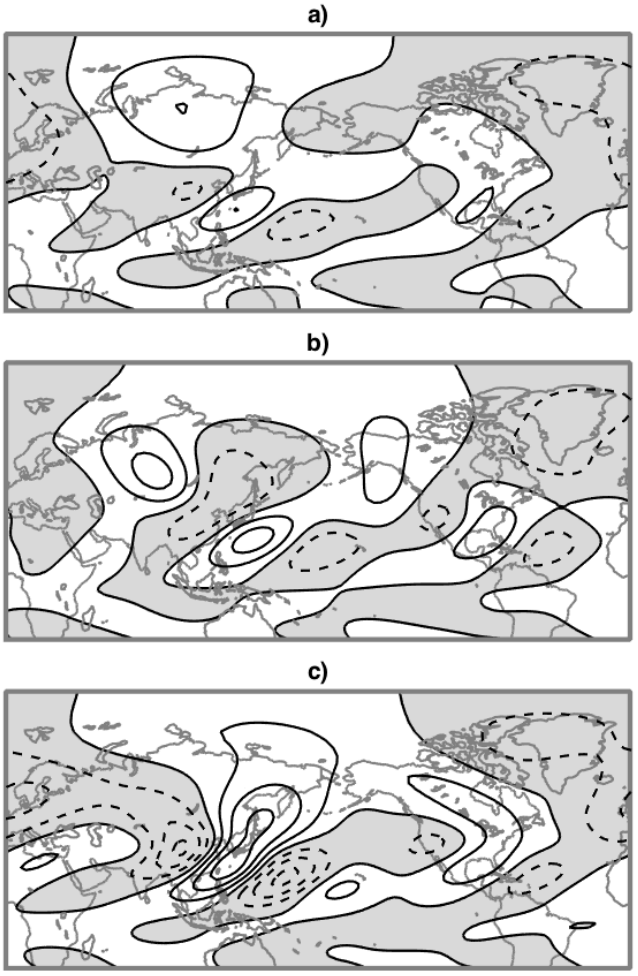

FIGURE 2.4: Winter (DJF) upper-level ($\sigma = 0.257$) stationary wave field in asymmetric streamfunction ($6 \times 10^6\ m^2 s^{-1}$ contours), from SWM basic state run with (a) control climatological period (1981-2000) basic state, (b) 2009/10 basic state, (c) 2013/14 basic state. (a)-(c): Solid contours indicate positive streamfunction, dashed contours and grey shaded areas indicate negative streamfunction.

2.2.3 Basic state ghost waves

When running the stationary wave model with the zonal mean basic state only (all four asymmetric forcings excluded) the stationary wave field generated is nonzero. Because there is no physical explanation for the zonal mean basic state to force

stationary waves (as these arise from zonal asymmetries per definition), this result indicates a model error. The basic state 'ghost waves' generated are consistent between runs, but depend on the choice of basic state. For instance, as seen in Figure 2.4, the 2009/10 and 2013/14 basic states generate more pronounced ghost waves than those of the climatological basic state. The presense of the ghost waves prevents the stationary wave patterns, generated when running the model with the four asymmetric forcings seperatly, from adding linearly to the full field, as the faulty basic state contribution gets 'counted' four times in the addition.

After careful consideration we have decided to remove the basic state ghost waves from the stationary wave output for all model simulations in this study (Figure 2.2 included), by subtracting out the ghost wave field corresponding to the basic state used. Removing the ghost waves does change the simulated stationary wave magnitudes and positions slightly, but does not alter the main results or conclusions. The general agreement between the climatological winter stationary wave decomposition in this study (Figure 2.2) and this same decomposition seen in previous studies, such as Wang and Ting (1999) and Held et al. (2002) (as argued in section 2.2.1), indicates that our results are valid when removing the basic state ghost waves.

Chapter 3

The 2009/10 and 2013/14 stationary wave fields

Before investigating the role of individual forcing mechanisms for specific winter seasons further, it is necessary to check how well the stationary wave model is able to reproduce the main features of the observed midlatitude stationary wave patterns in 2009/10 (December 2009 to February 2010) and 2013/14 (December 2013 to February 2014). This will be done by comparing the 2009/10 and 2013/14 stationary wave anomalies simulated by the model (Figure 3.1a,b) to the stationary wave anomalies from reanalysis data (Figure 3.1c,d).

3.1 Winter of 2009/10

For 2009/10, an overall weakening of the midlatitude climatological stationary wave field is seen in the reanalysis data (Figure 3.1c). Negative anomalies over climatological ridges and positive anomalies over climatological troughs indicate a weakened climatological pattern. A pronounced weakening of the North American trough and the Atlantic ridge is especially apparent, but there is also a noticeable weakening of the Pacific quadrapole pattern, including a slight eastward shift of the northeast center of the quadrapole. As seen by comparing Figure 3.2a with Figure 3.1c, the anomaly features in the North American region are consistent between different reanalysis data sets, though the weakening of the North American ridge appears to be more pronounced in ERA-Interim. (Note that ERA-Interim is

gridded at a higher resolution than NCEP-NCAR, and that Figure 3.2a,b displays December to March streamfunction anomalies at 500hPa, while Figure 3.1c,d displays December to February streamfunction anomalies at 250hPa. The anomalies are therefore not directly comparable).

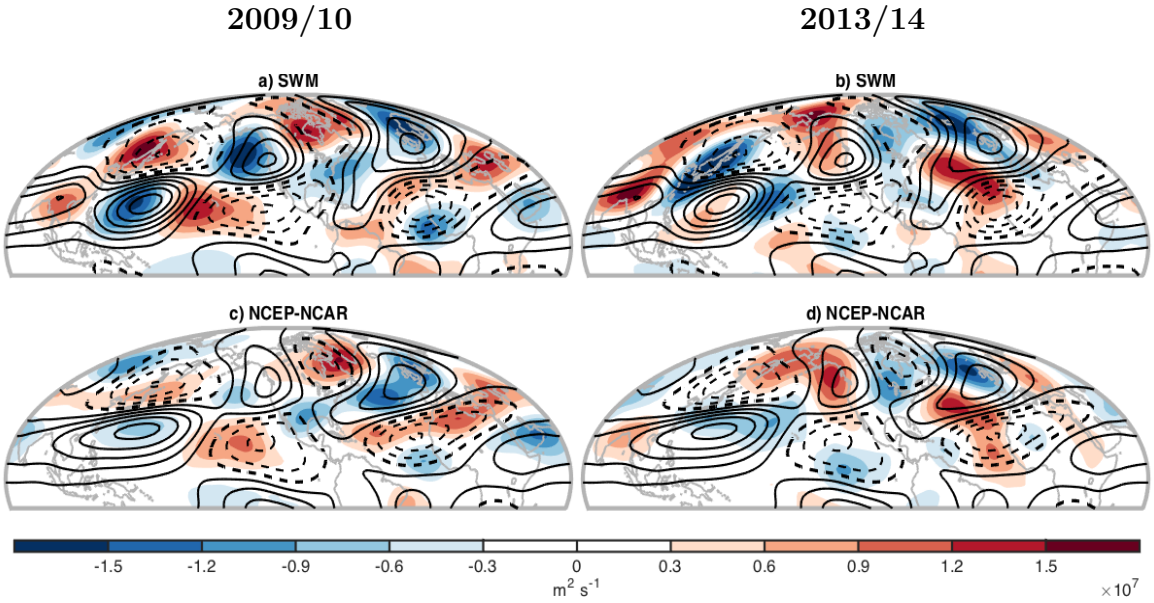

FIGURE 3.1: (a)-(b): Winter (DJF) upper-level ($\sigma = 0.257$) stationary wave anomalies (shadings) relative to the climatological control period (1981-2000; $6 \times 10^6 m^2 s^{-1}$ contours) in asymmetric streamfunction, from SWM simulations. (c)-(d): Winter (DJF) upper-level (250hPa) stationary wave anomalies (shadings) relative to the climatological control period (1981-2000; $6 \times 10^6 m^2 s^{-1}$ contours) in asymmetric streamfunction, from NCEP-NCAR reanalysis. (a)-(c): Solid contours indicate positive streamfunction, dashed contours indicate negative streamfunction.

The stationary wave model reproduces the weakening of the midlatitude climatological stationary wave pattern seen in reanalysis reasonably well. The weakening of the Atlantic ridge is captured particularly well by the model (Figure 3.1a), as the magnitude and position of the negative anomaly over the North Atlantic are very similar to what reanalysis data indicate. Also the weakening of the North American trough is captured by the model, but the shape of the anomaly is slightly different from reanalysis. This difference, however, is consistent with the difference in the shape of the climatological North American trough in the model compared to reanalysis. The model reproduces the weakening of the Pacific quadrapole pattern, but the anomaly magnitudes are exaggerated compared to reanalysis. Especially noticeable is the considerable weakening of the climatological North American ridge in the model simulation, which is not present in reanalysis to the same extent. This difference in the anomaly magnitude is consistent with the

climatological North American ridge being overly strong in the model simulation compared to reanalysis. Still, the model accurately reproduces the eastward shift of the northeast center of the Pacific quadrapole seen in reanalysis.

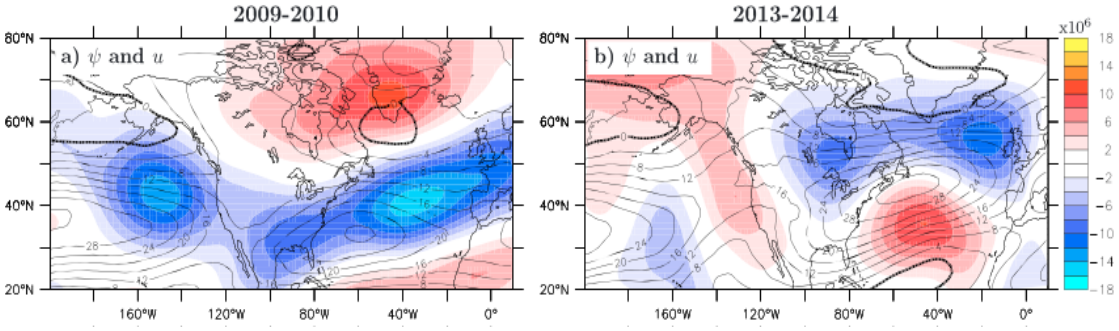

FIGURE 3.2: Winter (Dec-Mar) upper-level (500hPa) stationary wave anomalies (shadings; units m^2s^{-1}) in asymmetric streamfunction, and zonal wind (contours; $4ms^{-1}$), from ERA-Interim reanalysis (Riviére and Drouard, 2015).

As seen in Figure 3.2a the weakened stationary waves of 2009/10 are associated with a more zonal large-scale flow. For instance the weakened Atlantic ridge coincides with a more zonal, equatorward shifted Atlantic jet, while the weakened North American ridge allows for an eastward extension of the Pacific jet.

3.2 Winter of 2013/14

For 2013/14, an overall strengthening of the climatological North American ridge-trough pattern is seen in the reanalysis data (Figure 3.1d). Positive anomalies over climatological ridges and negative anomalies over climatological troughs indicate a strengthened stationary wave pattern. Looking at the stationary wave field for 2013/14 in reanalysis, a strengthened and northwest elongated North American ridge is present, in addition to a strengthened North American trough. Over the Atlantic, a northeast weakening and southwest strengthening of the climatological Atlantic ridge is visible. As seen by comparing Figure 3.2b with Figure 3.1d, these anomaly features are consistent between different reanalysis data sets, though the shape of the positive anomaly strengthening the North American ridge looks slightly different in ERA-Interim, with a maxima located further northwest.

For 2013/14, the stationary model reproduces the strengthening of the North American pattern seen in reanalysis well. The positive anomaly strengthening the North American ridge is captured by the model (Figure 3.1b), but the magnitude

is exaggerated and the anomaly maxima is shifted northwest compared to reanalysis (Figure 3.1d). A possible explanation for this discrepancy is related to the difference in the climatological pattern over the Bering Strait region between the model (where the streamfunction is negative) and reanalysis (where the streamfunction is positive). Due to bias in the model over this region, the response to local SSTs (Figure 1.2b) and related diabatic heating anomalies (Figure 1.3b) is exaggerated. The position and magnitude of the negative anomaly strengthening the North American trough is very well reproduced, with a maximum over the North Atlantic and extending west over southern Greenland into eastern North America. Over the Atlantic, the northeast weakening and southwest strengthening of the Atlantic ridge seen in reanalysis is captured particularly well by the model. Over the western North Pacific a strong negative anomaly is present in the model simulation, strengthening the climatological trough in this region. This feature is not present in reanalysis, and is therefore a noticeable difference between the stationary wave field produced by the model and the reanalysis data.

As seen in Figure 3.2b, the strengthened stationary waves over North America in 2013/14 are associated with a more wavy large-scale flow. In contrast to 2009/10, the strong North American ridge appears to deflect the Pacific jet polewards in the jet exit region, while over the Atlantic the northeast weakening and southwest strengthening of the Atlantic ridge is associated with a southwest-northeast tilt of the Atlantic jet. These features are discussed in more detail in Riviére and Drouard (2015), who show that large-scale circulation anomalies in the North Pacific influence the position of the Atlantic jet through synoptic wave breaking over North America and synoptic eddy feedback onto the mean flow.

Chapter 4

Forcing responses

In this chapter, the different forcing factors and their contributions to the circulation anomalies associated with the record-breaking winter weather of 2009/10 and 2013/14 will be explored in detail. Only upper-level December to February stationary wave responses will be discussed, as winter circulation and the jet level response is the focus of this study. In the following text, 'response' refers to the difference between the model run of a particular forcing experiment and the corresponding climatological run.

4.1 Winter of 2009/10

For 2009/10, the overall weakening of the climatological stationary wave pattern seen in reanalysis is captured well by the model, despite some minor discrepancies in the magnitude of the anomalies. When analyzing the results, we are interested in the forcing or forcing combination contributing to the main midlatitude stationary wave anomaly features for this winter season, namely, the weakened Atlantic ridge and the weakened North American ridge-trough pattern seen in Figure 3.1a.

Figure 4.1 shows the 2009/10 stationary wave responses to the different forcing experiments described in Table 2.1. The full stationary wave response to the 2009/10 forcings is seen in Figure 4.1a, and is a reproduction of the anomaly field (shadings) seen in Figure 3.1a. Figure 4.1b - e display the stationary wave responses to the four asymmetric forcings separately, and will be discussed in

detail in section 4.1.1. Figure 4.1f - o display the stationary wave responses to all possible combinations of the four forcing terms, and will be discussed in section 4.1.2.

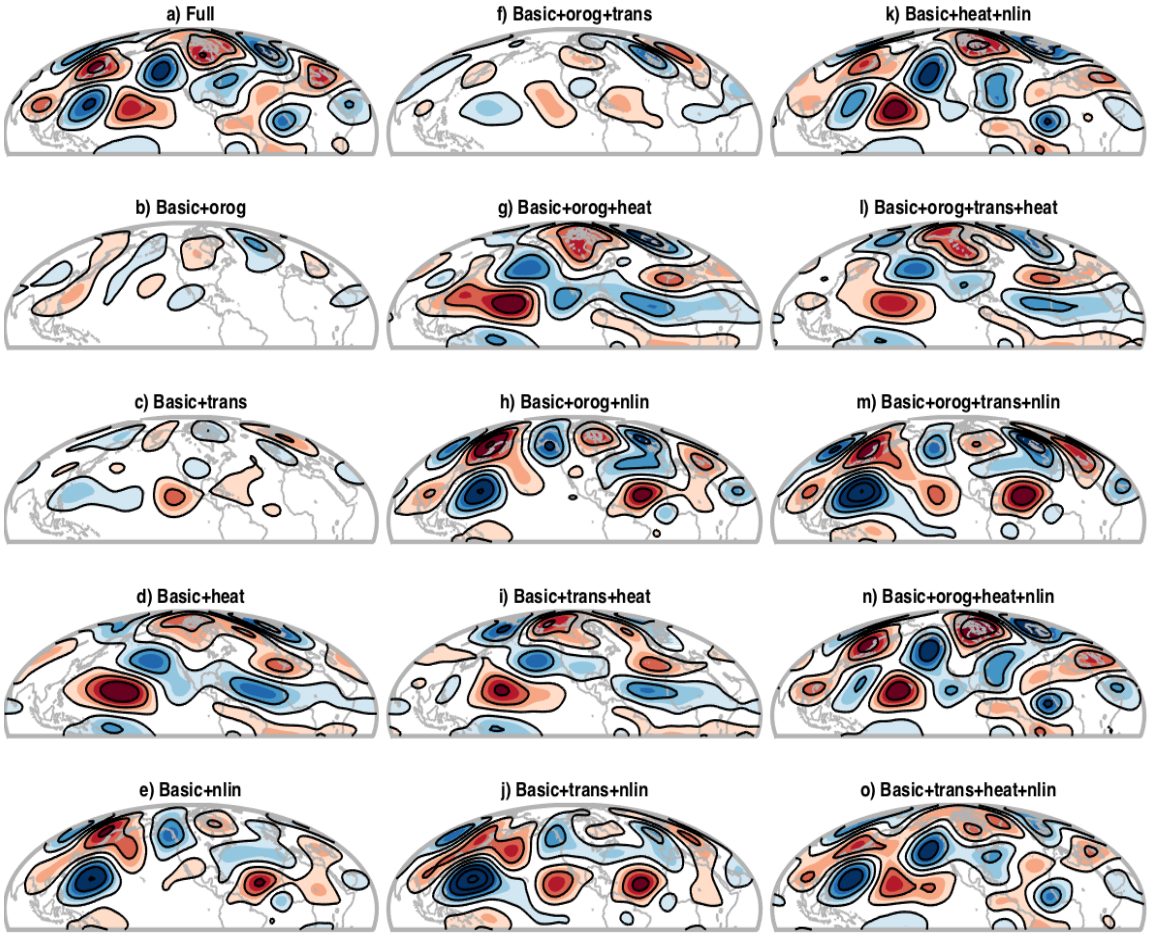

FIGURE 4.1: Winter (DJF) upper-level ($\sigma = 0.257$) 2009/10 stationary wave responses (contouring starts at $\pm 3 \times 10^6 m^2 s^{-1}$ with $6 \times 10^6 m^2 s^{-1}$ contour interval, shadings starts at $\pm 3 \times 10^6 m^2 s^{-1}$ with $3 \times 10^6 m^2 s^{-1}$ shading interval) in asymmetric streamfunction, from SWM forcing experiments. Blue shadings indicate negative response and red shadings indicate positive response.

4.1.1 Single forcings

The linear response to orography is relatively weak, but contributes noticeably to the overall weakening of the Atlantic ridge and the North American trough (Figure 4.1b). Note that with our experimental set-up, orography in itself is time-invariant, but the effect of the orographic forcing depends on the zonal mean basic state about which the model is linearized. The linear response to orography seen in Figure 4.1b therefore shows the effect of the 2009/10 zonal mean background flow over orographic features compared to that of the climatological zonal mean

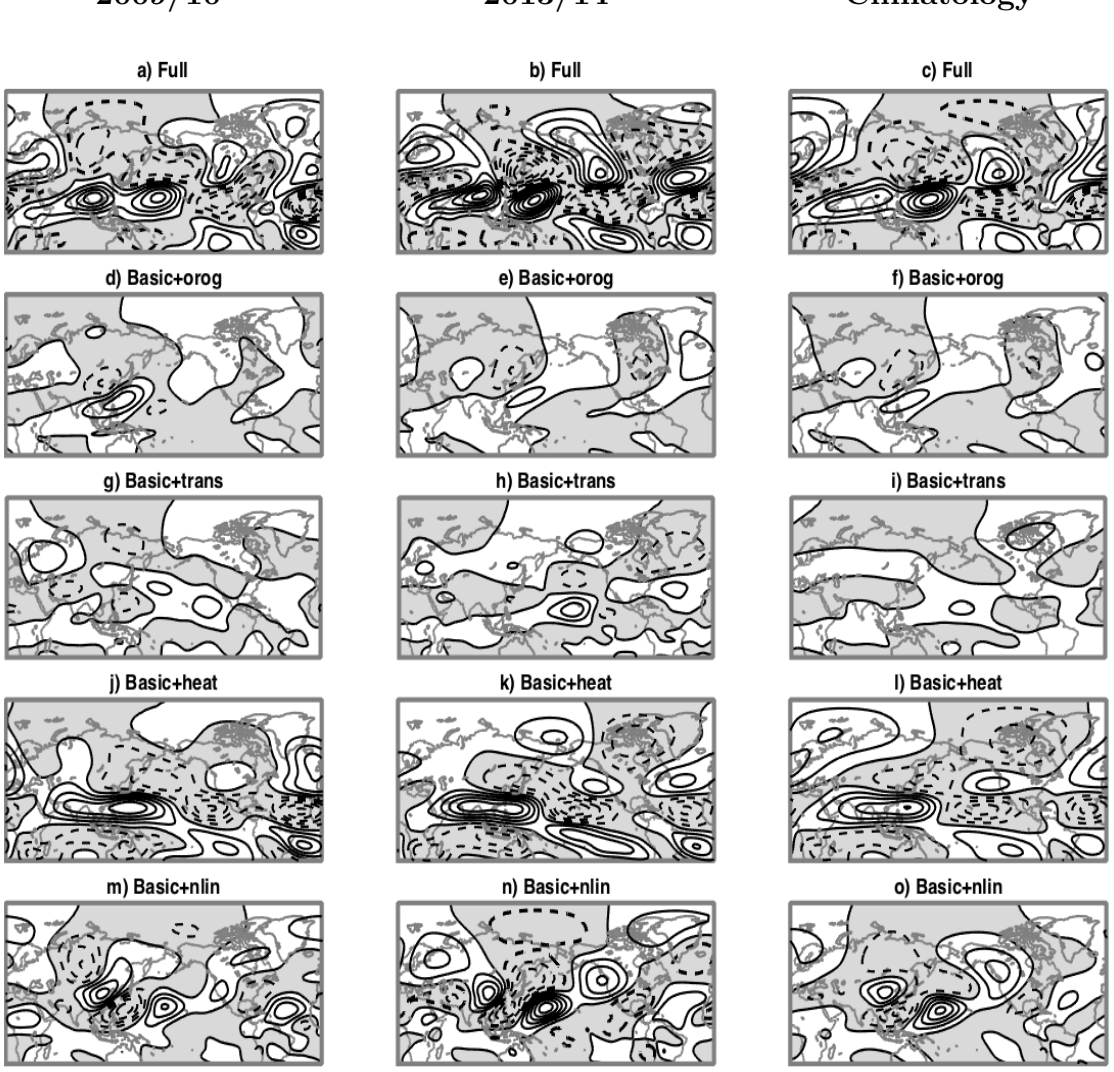

FIGURE 4.2: Decomposition of the 2009/10, 2013/14 and climatological control period (1981-2000) winter (DJF) upper-level ($\sigma = 0.257$) stationary wave fields ($6 \times 10^6 m^2 s^{-1}$ contours) in asymmetric streamfunction, from SWM. Solid contours indicate positive streamfunction, dashed contours and grey shaded areas indicate negative streamfunction.

background flow over orographic features. The orographic response in the North American/Atlantic sector (Figure 4.1b) is the result of less pronounced stationary waves downstream of the Rocky Mountains in 2009/10 (Figure 4.2d) compared to climatology (4.2f). The negative response over the North Atlantic contributes to the weakened Atlantic ridge seen in the full response, while the positive response over central North America contributes to the weakened North American trough seen in the full response. The orographic response in the Pacific sector (Figure 4.1b) is the result of an enhanced wave-train downstream of the Tibetan Plateau in 2009/10 (Figure 4.2d) compared to climatology (Figure 4.2f). The orographic forcing is sensitive to changes in the low-level mean flow, and more pronounced

stationary waves are generally forced by stronger low-level zonal mean winds (Held and Ting, 1990). As seen in Figure 4.3c the low-level zonal mean wind in the Pacific region (120°E-110°W) at 20-40°N latitude is stronger than climatology, and can therefore partially explain the enhanced wave-train in 2009/10 and consequently the Pacific response to orography.

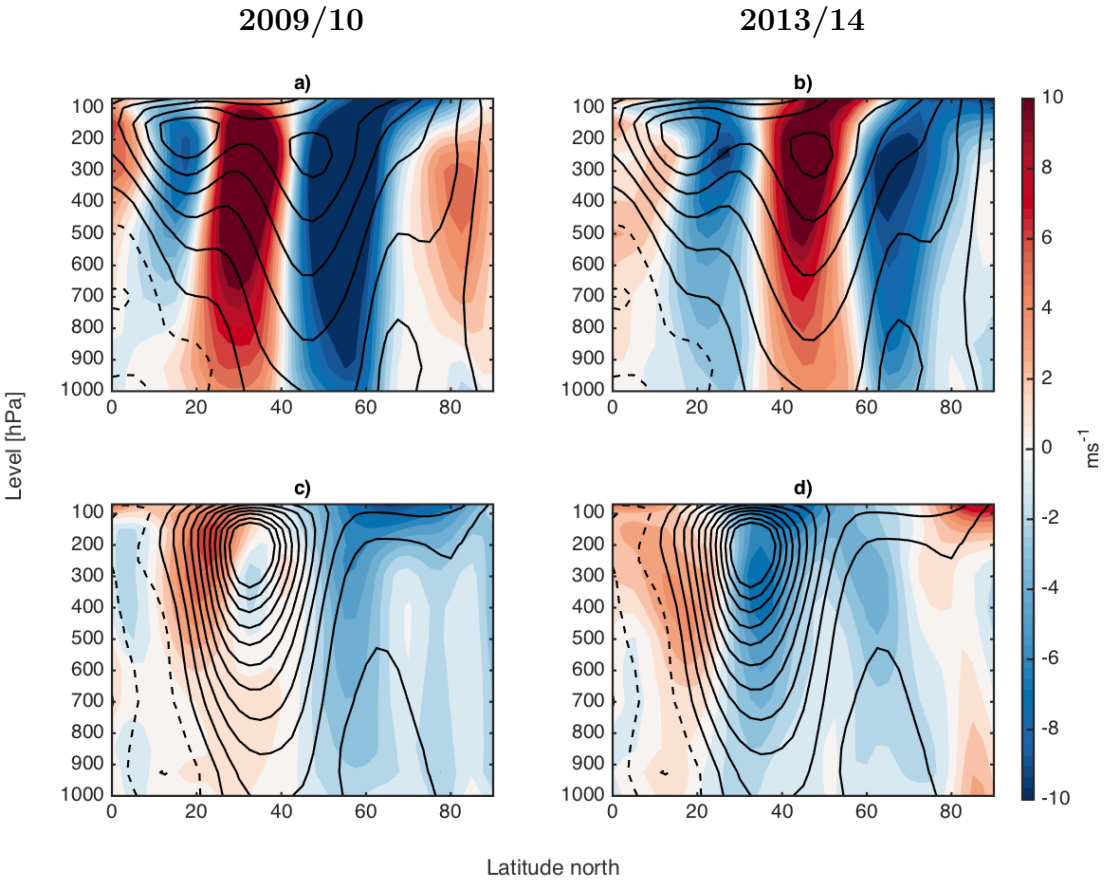

FIGURE 4.3: (a)-(b): Winter (DJF) zonal mean zonal wind anomaly (shadings) over the Atlantic sector (90°W-40°E) relative to the climatological control period (1981-2000; contours $5ms^{-1}$), from NCEP-NCAR reanalysis. (c)-(d): Winter (DJF) zonal mean zonal wind anomaly (shadings) over the Pacific sector (120°E-110°W) relative to the climatological control period (1981-2000; contours $5ms^{-1}$), from NCEP-NCAR reanalysis.

The linear response to diabatic heating is particularly strong over the Pacific Ocean during this winter, and is likely connected to the deep tropical heating associated with an El Niño event. The total response to diabatic heating (Figure 4.1d) strongly resembles the results of Ting (1996) forcing a linear baroclinic model, similar to the one used in this study, with an idealized tropical heat source imitating that of an El Niño event (Figure 4.4). This similarity indicates that the El Niño event is likely a dominant factor in the total diabatic heating response this winter, not only in the tropical Pacific, but also over the Atlantic and for higher

latitudes. El Niño related heating generally leads to upper-level divergence locally, accompanied by a strong anticyclonic anomaly pair centered slightly west of the heating, and a weaker cyclonic anomaly pair further east (Ting, 1996). This is consistent with the Pacific response to diabatic heating seen in Figure 4.1d, with a strong anticyclonic anomaly pair over the central tropical Pacific located in the same region as the heating anomalies seen in Figure 1.3a, which likely originate from the warm tropical SST anomalies seen in Figure 1.2a centered slightly east of this heating response. Over the North Pacific, the diabatic heating response contributes to the overall weakening of the North American ridge, while also compressing the ridge meridionally. Additionally, the diabatic heating response is a major contributor to the overall weakening of the North American trough, with an extensive positive response over Alaska and Canada. In the Atlantic sector the diabatic heating response contributes to a northeast weakening and a southwest strengthening of the Atlantic ridge, as opposed to the overall weakening seen in the full response (Figure 4.1a).

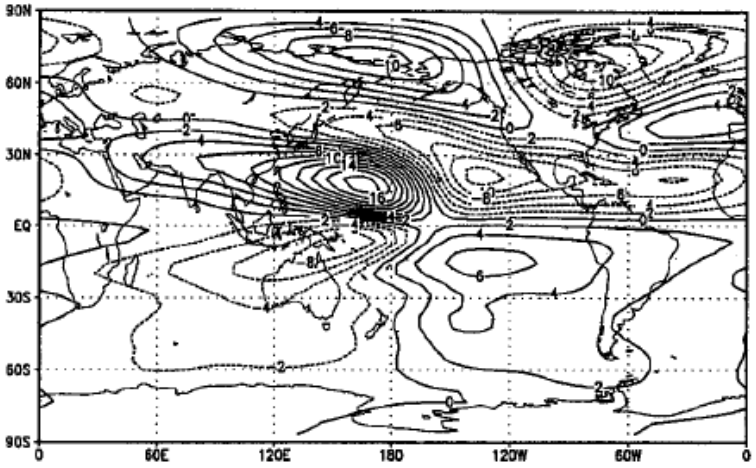

FIGURE 4.4: Winter (DJF) upper-level (200hPa) linear baroclinic model response ($2 \times 10^6 m^2 s^{-1}$ contours) to a steady tropical heat source centered at 0° latitude and 180° longitude, in asymmetric streamfunction (Ting, 1996).

The linear response to transient eddies is relatively weak, and acts to counteract the overall weakening of the North American ridge-trough pattern, but reinforces the overall weakening of the tropical Pacific pattern. The positive response over Alaska and the negative response over Greenland seen in Figure 4.1c have a strengthening effect on the North American ridge-trough pattern, as opposed to the overall weakening seen in Figure 4.1a. In the tropical Pacific, the transient response contributes to the overall weakening of the climatological pattern seen in

Figure 4.1a. The negative response to transient eddies over the western tropical Pacific approximately collocates with the positive response to diabatic heating in that same region. This is consistent with what was found in Ting and Held (1990), where transients were shown to dampen the response to tropical SST anomalies locally.

The stationary nonlinear response is an important contributor to the overall weakening of the North American ridge-trough pattern, while also contributing to the overall weakening of the Atlantic ridge. The stationary nonlinear term accounts for nonlinear interactions between the background flow and the asymmetric forcings, as well as interactions between the different asymmetric forcings. The negative response over the North American west coast seen in Figure 4.1e is a consequence of the 2009/10 North American ridge forced by stationary nonlinearity (Figure 4.2m) being considerably weaker than the climatological ridge forced by stationary nonlinearity (Figure 4.2o). The North American ridge is maintained mainly by nonlinear interactions between flows forced by diabatic heating and flows forced by the Rocky Mountains (Ringler and Cook, 1999; Ting et al., 2001). A weak North American ridge indicates that these interactions generated weaker stationary waves in 2009/10 compared to the climatological control period. The negative response over the North Atlantic contributes to the overall weakening of the Atlantic ridge, and could possibly be related to nonlinear interactions between transient eddies and the background flow in the Atlantic sector, as suggested by Riviére and Drouard (2015). The stationary nonlinear response is also important for the overall weakening of the western Pacific pattern, with a strong negative response present in the western tropical Pacific and a strong positive response to the north (Figure 4.1e). This pattern counteracts the diabatic heating response in that same region (Figure 4.1d), and consequently shifts the diabatic heating response eastward (Figure 4.1k).

4.1.2 Combined forcings

The combined response to diabatic heating and stationary nonlinear forcing (Figure 4.1k) accurately captures nearly the entire stationary wave anomaly field seen in the full response (Figure 4.1a). Diabatic heating and stationary nonlinearity reinforce each other in the North American and North Atlantic region, creating a

pronounced weakening of the North American ridge-trough and the Atlantic ridge. The stationary nonlinearity term dominates the western Pacific response, and contributes to shifting the El Niño related wave-train seen in Figure 4.1d eastward. When comparing the combined response to diabatic heating and stationary nonlinearity (Figure 4.1k) to the combined response to diabatic heating, stationary nonlinearity and transients (Figure 4.1o), it is clear that the transient eddies act to counteract the overall weakening of the Atlantic ridge and the North American ridge. Orography, on the other hand, reinforces the effect of diabatic heating and stationary nonlinearity in this same region (Figure 4.1n).

The results suggest that El Niño related SST anomalies were likely a major driver of the stationary wave anomalies in 2009/10, through the diabatic heating forcing. Also nonlinear interactions between the different forcings of stationary waves were important this winter. However, it is not unlikely that the considerable heating anomalies present in the tropical Pacific could be important in altering these interactions and consequently contribute to stationary wave anomalies through the nonlinear term, as diabatic heating related nonlinear effects have been shown to be the largest contributor to the fully nonlinear response (Sobolowski et al., 2011).

4.2 Winter of 2013/14

For 2013/14, the overall strengthening of the climatological North American pattern seen in reanalysis is reproduced quite well by the model, even though the magnitude of the North American ridge anomaly is slightly exaggerated. This winter we are especially interested in the forcing factors contributing to strengthening the climatological North American ridge-trough pattern, as well as the southwest strengthening and northeast weakening of the climatological Atlantic ridge, as seen in Figure 3.1b.

Figure 4.5 shows the 2013/14 stationary wave responses to the different forcing experiments described in Table 2.1. The full stationary wave response to the 2013/14 forcings is seen in Figure 4.5a, and is a reproduction of the anomaly field (shadings) seen in Figure 3.1b. Figure 4.5b - e display the stationary wave responses to the four asymmetric forcings separately, and will be discussed in detail in section 4.2.1. Figure 4.5f - o display the stationary wave responses to all

possible combinations of the four forcing terms, and will be discussed in section 4.2.2.

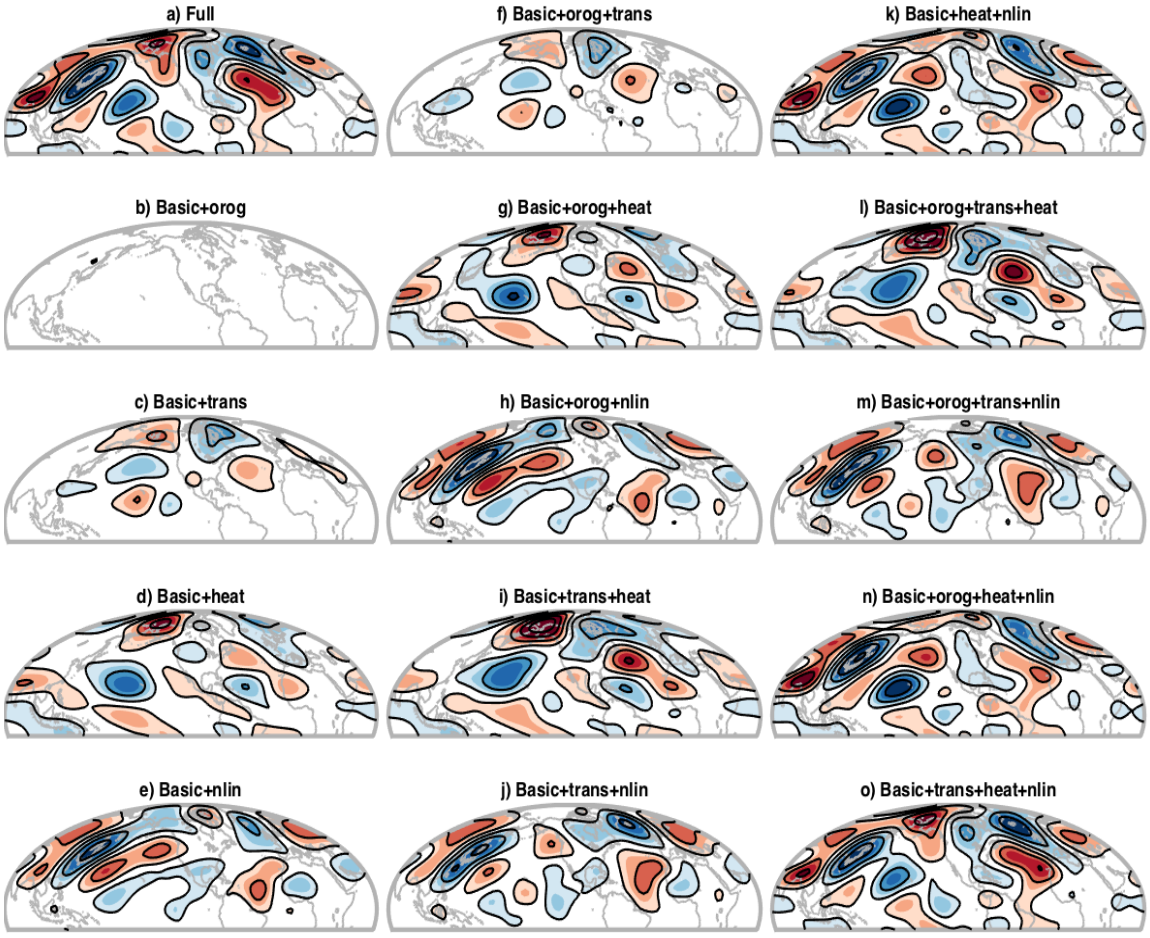

FIGURE 4.5: Winter (DJF) upper-level ($\sigma = 0.257$) 2013/14 stationary wave responses (contouring starts at $\pm 3 \times 10^6 m^2 s^{-1}$ with $6 \times 10^6 m^2 s^{-1}$ contour interval, shadings starts at $\pm 3 \times 10^6 m^2 s^{-1}$ with $3 \times 10^6 m^2 s^{-1}$ shading interval) in asymmetric streamfunction, from SWM forcing experiments. Blue shadings indicate negative response and red shadings indicate positive response.

4.2.1 Single forcings

The linear response to orography is considerably weaker than the other forcing responses this winter, and is barely visible in Figure 4.5b. This suggests that the stationary wave field generated by orography in 2013/14 (Figure 4.2e) is quite similar to that of climatology (Figure 4.2f). However, the weak response does not necessarily mean that orography is unimportant in forcing stationary wave anomalies in 2013/14. Above a critical height, defined as the mountain height where the magnitude of the terms discarded during linearization will be comparable to the retained terms, the linear approximation will no longer be valid. According to

Ringler and Cook (1997) the exact critical height will depend on the relationship between surface wind speeds, wind shear and meridional temperature gradients, but generally the Tibetan Plateau and the Rocky Mountains are expected to give a nonlinear contribution. This implies that orography may still have an important role in 2013/14, but its influence will be embedded in the stationary nonlinearity response and not in the linear orographic response.

Diabatic heating is again an important forcing of stationary wave anomalies this winter, with a strong positive response centered over the Bering Strait being a major contributor to the overall strengthening of the North American ridge (Figure 4.5d). Over the North Atlantic, the diabatic heating response contributes to the overall southwest strengthening - northeast weakening of the Atlantic ridge seen in Figure 4.5a. Additionally, diabatic heating appears to be the main source of the negative response over the central Pacific seen in the full response field. The diabatic heating response in Figure 4.5d is structurally similar to the circulation anomalies found in Hartmann (2015) by regressing 500hPa 1979-2014 November to March geopotential height anomalies onto the North Pacific mode (EOF-2 of global SST) (Figure 4.6). This indicates that large parts of the diabatic heating response, such as the negative response over the central Pacific, the positive response strengthening the North American ridge, and the North Atlantic response, were possibly due to SST anomalies associated with a positive phase of the North Pacific mode this winter. Specifically, it is the North Pacific warm SST anomalies seen in Figure 1.2b that are thought to have driven this response, which likely originate from warm SSTs in the western tropical Pacific.

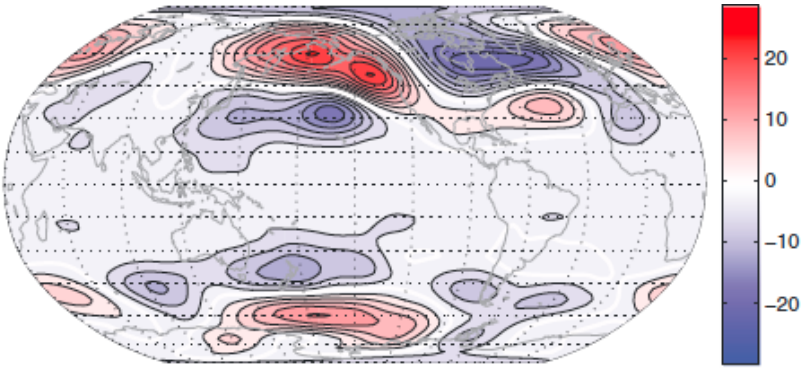

FIGURE 4.6: Regression of the 1979-2014 winter (Nov-Mar) 500hPa geopotential height anomalies [3m contours] from NCEP-NCAR reanalysis onto the principal component time series for the second EOF of global SST for the period 1979-2014 (Hartmann, 2015).

The linear response to transient eddies is relatively weak, but contributes noticeably to the overall strengthening of the North American ridge-trough pattern, with a negative response over Greenland and northeastern North America, and a positive response over Alaska (Figure 4.5c). The negative response in the North Atlantic region, with a positive response to the south, could be related to a poleward shift of the storm tracks this year. In accordance with Riviére and Drouard (2015), the Atlantic response seen in Figure 4.5c suggests that transient eddies in 2013/14 contributed to shifting the Atlantic jet poleward, and thus inducing a positive NAO phase.

The response to the stationary nonlinear forcing is relatively strong, especially in the western Pacific region, and acts to dampen the overall strengthening of the North American trough, in addition to limiting the overall northwest elongation/strengthening of the North American ridge. The split wave-train over the Pacific seen in Figure 4.5e emerges downstream of the Tibetan Plateau, and even though we cannot specifically determine which nonlinear interactions are dominating this response, it is likely that orography plays an important part here.

4.2.2 Combined forcings

The combined response to diabatic heating and transient forcing (Figure 4.5i) accurately captures large parts of the North American and North Atlantic stationary wave anomaly field seen in the full response (Figure 4.5a). Diabatic heating and transient forcing reinforce each other in the North American and North Atlantic region, creating a pronounced strengthening of the North American ridge-trough and a northeast weakening - southwest strengthening of the Atlantic ridge. Comparing the combined effect of transients and diabatic heating (Figure 4.5i) to the combined effect of transients, diabatic heating and stationary nonlinearity (Figure 4.5o), it is clear that stationary nonlinearity is important in shaping the North American ridge anomaly, as well as the western Pacific response, via the pronounced wave-train downstream of the Tibetan Plateau seen in Figure 4.5e.

The results suggest that SST anomalies related to a positive phase of the North Pacific mode were an important driver of the 2013/14 stationary wave anomalies, through the diabatic heating forcing. Transient eddies reinforce this effect,

resulting in an amplified wave pattern over North America this winter. Nonlinear interactions were important in adjusting the shape and magnitudes of stationary wave anomalies already produced by diabatic heating and transient eddies combined.

4.3 Summary

For both 2009/10 and 2013/14, diabatic heating was an important driver of winter circulation anomalies, with heating anomalies likely connected to patterns of natural variability in Pacific SSTs: an El Niño event in 2009/10 (EOF-1 of global SST), and a positive phase of the North Pacific mode in 2013/14 (EOF-2 of global SST). The different SST anomaly patterns result in slightly different stationary wave responses to diabatic heating, with a stronger and sligthly poleward shifted response in 2009/10 compared to 2013/14. Interestingly, transient eddies act to dampen the heating response in 2009/10, but reinforce the heating response in 2013/14. In 2013/14, the transient forcing was particularly important in strengthening the North American trough, something that was possibly related to a poleward shift of the Atlantic storm tracks this winter. Nonlinear interactions were important both winters, but the 2009/10 and the 2013/14 stationary nonlinearity response fields look quite different, especially in the western Pacific region. However, stationary nonlinearity appears to have had a weakening effect on the climatological Atlantic ridge and the climatological North American trough both winters.

Chapter 5

Discussion and conclusions

The 2009/10 and 2013/14 winter circulation anomalies, and the forcing factors driving them, were analyzed using a linear stationary wave model. Our results show that none of the four asymmetric forcings can alone fully explain the circulation anomalies observed in 2009/10 and 2013/14. Still, large parts of the anomaly fields were forced by diabatic heating, combined with stationary nonlinear effects in 2009/10, and transient forcing in 2013/14. In this chapter, the implications of these results are discussed further, limitations to our approach will be addressed, directions for future studies put forward, and concluding remarks provided.

5.1 Origins of variability and mechanistic pathways

The weakened stationary wave pattern seen in 2009/10 was associated with a zonalized large-scale flow, while the strengthened stationary wave pattern over North America in 2013/14 was associated with a more wavy large-scale flow. In this section, the results will be discussed in the context of possible driving mechanisms of the diabatic heating patterns, such as Pacific SST variability and Arctic sea ice loss, which may have contributed to these differences in the 2009/10 and 2013/14 midlatitude winter circulation.

5.1.1 Pacific SST variability

Diabatic heating is found to be a particularly important forcing of circulation anomalies in both the 2009/10 and 2013/14 winter seasons, although it cannot alone explain the seasonal anomalies completely. Generally, large parts of the year-to-year variability in diabatic heating come from SST variability. A number of studies have shown tropical SST anomalies to force considerable atmospheric circulation anomalies, not only in the tropics, but also in midlatitude regions (Hoskins and Karoly, 1981; Palmer and Mansfield, 1984; Ting and Held, 1990). Midlatitude SST anomalies, typically driven by atmospheric anomalies, have also been shown to create circulation anomalies, though generally of modest magnitude compared to internal atmospheric variability (Kushnir et al., 2002). In this study, the main effect of the SST anomalies seen in 2009/10 and 2013/14 (Figure 1.2a,b) is embedded in the diabatic heating responses, as they have the potential to alter the sensible and latent heat fluxes at the ocean-atmosphere interface. Based on the findings of Ting (1996) (Figure 4.4) and Hartmann (2015) (Figure 4.6) (as argued in section 4.1.1 and 4.2.1 respectively), we suspect that natural variability in Pacific SSTs forces large parts of the stationary wave responses to diabatic heating in both years, with an El Niño event in 2009/10 (EOF-1 of global SST), and a positive phase of the North Pacific mode in 2013/14 (EOF-2 of global SST). The two patterns of variability force different responses; the 2009/10 diabatic heating response is generally stronger than that of 2013/14 (with the exception of the particularly strong ridge anomaly located over the Bering Strait in 2013/14), and appears to be more poleward shifted. Such differences are expected, as the magnitude of circulation anomalies forced by SST anomalies are roughly linearly dependent on the SST anomaly strength (Ting, 1991; Ting and Held, 1990), but also sensitive to the latitudinal and longitudinal position of the SST anomaly (Palmer and Mansfield, 1984).

This study does not explicitly investigate the origins of the 2009/10 and 2013/14 heating anomalies driving the diabatic heating responses directly, but the inferred connections to Pacific SST anomalies are supported by previous studies. In 2009/10, warm SSTs related to El Niño (Figure 1.2a) are likely an immediate cause of the strong central tropical Pacific diabatic heating anomalies seen in Figure 1.3a, consistent with the imposed deep, equatorial heat source seen in Ting (1996). The connection between SSTs and the diabatic heating field in 2013/14 is

less obvious. The region of exceptionally warm SSTs in the North Pacific this winter (Figure 1.2b) is not directly visible in the diabatic heating field (Figure 1.3b). However, a strong heating anomaly in the western tropical Pacific is apparent, which is likely due to moderately warm SST anomalies in this region increasing the already high SSTs of the Pacific warm pool and leading to atmospheric water loading and strong latent heat release (Palmer, 2014). As a result, we believe large parts of the diabatic heating response in 2013/14 are driven by these moderate SST anomalies in the western tropical Pacific associated with a positive phase the North Pacific mode. To explore the Pacific SST hypothesis directly, one could drive a GCM with the observed 2009/10 and 2013/14 tropical Pacific SST anomalies and study the circulation anomalies generated. To further determine the effect of these Pacific SST anomalies as a thermal forcing, the stationary wave model could be used to decompose the forcing field of the GCM output, using the same approach as shown in this study with reanalysis data.

5.1.2 Arctic sea ice loss

Dramatic changes are occurring in the Arctic climate system due to global warming, and Arctic sea ice loss is both a driver and a consequence of this change due to the snow-ice-albedo feedback and other feedback processes. Local effects of sea ice loss on the atmospheric circulation are well documented in both modeling and observational studies (e.g. Alexander et al., 2004, Deser et al., 2010, Jaiser et al., 2012), but the debate over whether reductions in Arctic sea ice extent can force midlatitude circulation anomalies is still ongoing (Barnes and Screen, 2015; Francis and Vavrus, 2015).

In this study, the potential effect of reduced Arctic sea ice on the atmospheric circulation in 2009/10 and 2013/14 is mainly embedded in the diabatic heating response, as sea ice loss typically induces low-level heating. Because natural variability in Pacific SSTs appears to account for such large parts of the total diabatic heating responses found both winters, it is likely that sea ice only contributes with a small and/or local effect. Additionally, the contrasting circulation patterns seen in the 2009/10 and 2013/14 winter seasons are suggestive of considerable interannual variability being present. This indicates that reduced Arctic sea ice, due to global warming, is likely not a dominant forcing of the 2009/10 and 2013/14

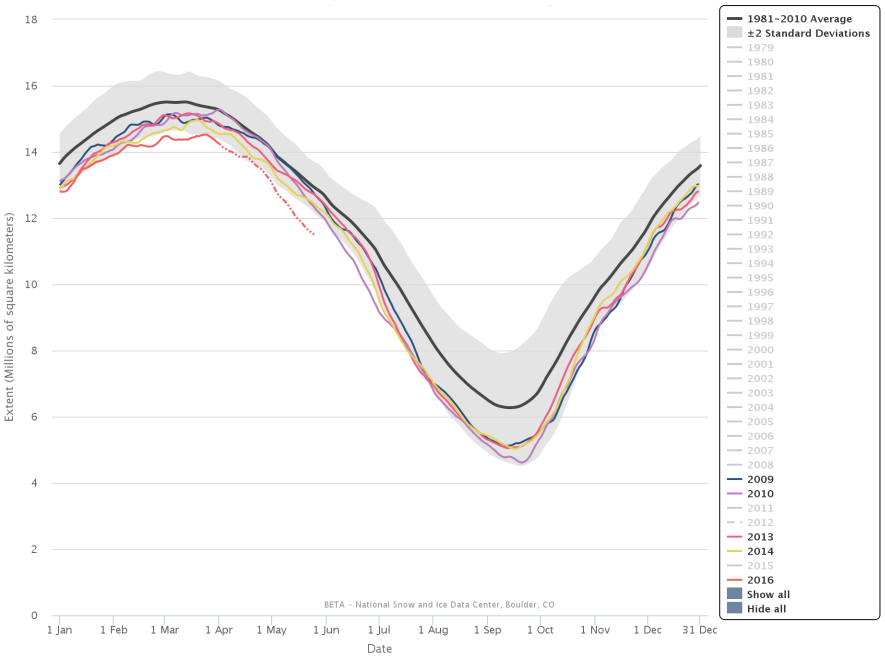

FIGURE 5.1: Seasonal cycle of Arctic sea ice extent in 2009 (blue), 2010 (purple), 2013 (pink), 2014 (yellow), 2016 (red), and the 1981-2010 average (black), from the National Snow and Ice Data center (retrieved at http://nsidc.org/arcticseaicenews/charctic-interactive-sea-ice-graph/)

circulation anomalies, as moderate losses of sea ice were present both years (Figure 5.1), with similar spatial patterns in early winter (Figure 5.2a,b) and more different patterns in late winter (Figure 5.2c,d). For 2013/14, our results show signs of a possible local response to sea ice loss - noticeable reductions in sea ice extent and concentration were present in the Bering Sea from December through February (not shown), and this would have contributed to the heating anomalies in the area (Figure 1.3b). These heating anomalies could potentially contribute to strengthening the upper-level ridge anomaly (likely produced mainly by Pacific SST anomalies) centered over the Bering Strait this winter (Figure 4.5d). Several studies present evidence suggesting that eddy-mean flow adjustments to the initial atmospheric response to sea ice changes also are important (e.g. Honda et al., 2009, Inoue et al., 2012, Jaiser et al., 2012). Such effects will in this study be embedded in the nonlinear and transient terms, but it is difficult to separate them from other nonlinear interactions (as discussed in section 5.2).

With the current approach, it is not possible to explicitly determine the effect of Arctic sea ice reductions on the large-scale atmospheric circulation during these winters. For future studies we recommend an experimental design where the 2009/10 and 2013/14 diabatic heating forcing is turned on/off in different latitude

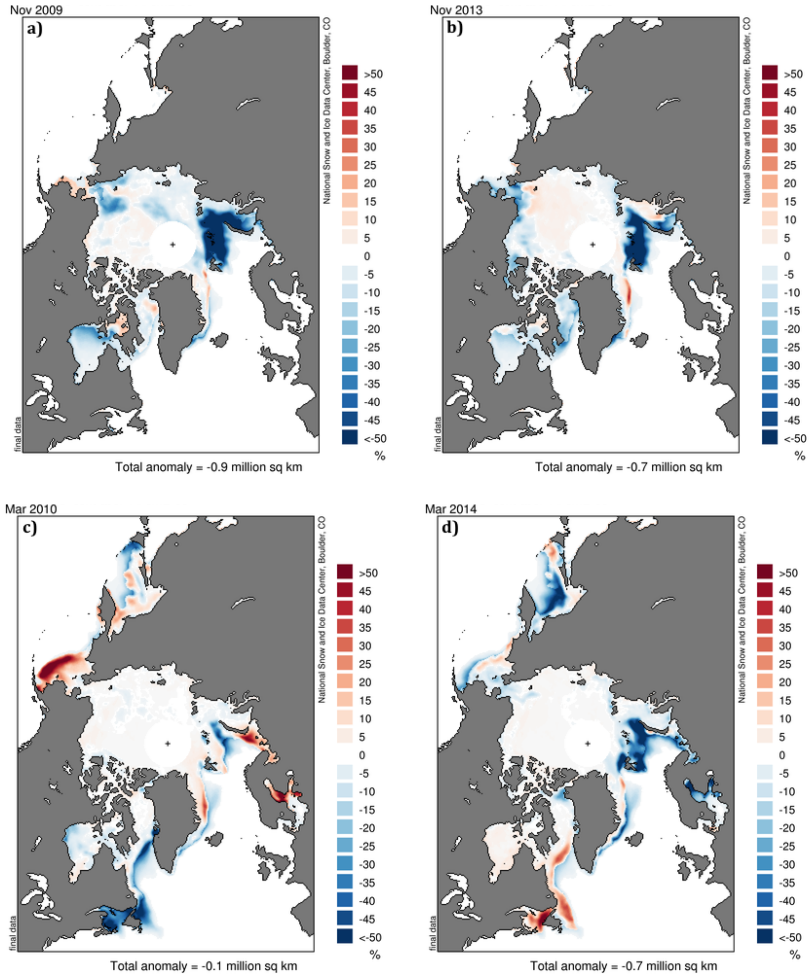

FIGURE 5.2: Sea ice concentration anomalies in (a) November 2009, (b) November 2013, (c) March 2010, and (d) March 2014 relative to climatology (1981-2010) from the National Snow and Ice Data center (retrieved at https://nsidc.org/data/bist/).

bands (e.g. tropics, midlatitudes, high-latitudes) to further explore the local/remote response to tropical diabatic heating compared to the local/remote response to Arctic diabatic heating (experiments for idealized Arctic heating anomalies not specific to a given season were performed by Sellevold (2015)). Such an experiment could more explicitly test the hypothesis that tropical heating anomalies, not sea ice reductions, were the main driver of the circulation response to diabatic heating in 2009/10 and 2013/14.

5.1.3 Potential teleconnection pathways to the midlatitudes

For tropical Pacific or Arctic diabatic heating anomalies to affect midlatitude circulation, there must be a pathway for communicating these signals over long

distances. Several possible pathways are discussed in this subsection.

A number of studies suggest that the stratosphere plays an important part in communicating circulation anomalies over the Pacific to the Atlantic region during El Niño winters, through the 'stratospheric bridge' teleconnection (e.g. Brönnimann, 2007, Ineson and Scaife, 2009). According to this hypothesis planetary waves generated by tropical SST anomalies propagate vertically, resulting in a weakened stratospheric polar vortex. A weak polar vortex typically favors a negative NAO phase, and can therefore affect the large-scale circulation over the North Atlantic (Perlwitz and Graf, 1995). Similar arguments have been made as a possible pathway for Arctic sea ice loss to affect midlatitude circulation, as newly ice-free regions in early winter have also been associated with a weakening of the stratospheric polar vortex and a negative NAO signal (Kim et al., 2014; King et al., 2015).

Our experimental set-up does not allow us to further explore the potential stratospheric connection between the Pacific and the Atlantic regions in 2009/10 and 2013/14. Based on the AO index (not shown), a weak stratospheric polar vortex was present in the winter of 2009/10 and in January of 2013/14, but we cannot infer causality between Pacific heating anomalies and the presence of a weak polar vortex. For future research we suggest forcing a model with a well-resolved stratosphere with the 2009/10 and 2013/14 Pacific heating anomalies, and study the stratospheric response as well as the tropospheric Atlantic response. Preferably a nonlinear model should be used, as the stratospheric pathway involves wave-driving arguments.

Another possible pathway involves tropospheric interactions between propagating planetary waves and the mean flow. This hypothesis is motivated by the fact that central Pacific El Niño winters (such as 2009/10) are reportedly associated with a less weakened stratospheric polar vortex than that of eastern Pacific El Niño winters, but are more strongly linked to a negative NAO circulation pattern (Graf and Zanchettin, 2012). Consequently, Graf and Zanchettin (2012) propose a 'tropospheric bridge' as the mechanism primarily responsible for establishing a negative NAO phase during central Pacific El Niño winters. The idea is that planetary waves generated in the tropical Pacific by anomalous SSTs are trapped by an eastward extended Pacific jet, causing them to propagate eastward within the

subtropical waveguide, resulting in a weakened Atlantic ridge typical for negative NAO conditions.

For 2009/10, the diabatic heating response found in our study is similar to the central Pacific El Niño response described in Graf and Zanchettin (2012), with a negative response (northeast of the tropical heating anomaly) that extends southeastward over the Atlantic and contributes to weakening the Atlantic ridge. Additionally, the Pacific jet is clearly extended eastward in 2009/10 (Figure 1.2e). These results suggest that the 'tropospheric bridge' is potentially an important pathway for tropical Pacific SST anomalies to affect Atlantic midlatitude circulation in 2009/10. In 2013/14, the Pacific jet is not extended eastward, but rather veers poleward in the jet exit region (Figure 1.2f), and the Atlantic response to diabatic heating is visibly weaker compared to 2009/10. This suggests that the 'tropospheric bridge' proposed by Graf and Zanchettin (2012) is not activated in 2013/14, because the subtropical wave guide is too weak. The importance of transient forcing and stationary nonlinearity to the Atlantic response seen in 2013/14 suggests that perhaps transient eddies interacting with the mean flow is a more important pathway this winter. This aspect will be discussed further in the following section.

5.2 Nonlinear interactions

In linear theory it is assumed that the atmosphere responds to each individual forcing of stationary waves separately, while in reality the atmosphere responds to the total forcing of diabatic heating, orography and transient eddies combined, something which includes nonlinear interactions between flows generated by the different forcing factors (Held et al., 2002). In this study, the stationary nonlinear forcing allows us to assess the importance of these nonlinear interactions even though they are not explicitly represented (nonlinear terms are neglected in the linearization of the model equations). Nonlinear interactions are found to be important both winters, but contribute to the 2009/10 and 2013/14 circulation anomalies differently. In 2009/10, stationary nonlinear forcing, together with diabatic heating, is found to drive the most important circulation anomalies. Contrastingly, in 2013/14, stationary nonlinearity is found to mainly adjust the

magnitudes and shape of the circulation anomalies set up by diabatic heating and transient eddy forcing.

The linear framework used in this study does not allow us distinguish between different nonlinear interactions and their relative contributions. This is a clear limitation to our approach, especially when considering that stationary nonlinear forcing does contribute noticeably to the midlatitude circulation anomalies seen in 2009/10 and 2013/14. The hypothesis of tropical SST anomalies driving these circulation anomalies (while sea ice loss is less important), is not necessarily less valid because nonlinear interactions are important; in fact parts of the true response to SST anomalies will be hidden in the nonlinear term and in the transient forcing, as SST anomalies for instance can alter the nature of eddy-mean flow interactions and change the storm tracks. For future studies we recommend utilizing a nonlinear stationary wave model that explicitly includes the effects of the nonlinear interactions seen in 2009/10 and 2013/14 respectively.

Still, some inferences can be made based on findings from previous studies. Ringler and Cook (1999) found that the presence of heating tends to reduce the magnitude of the orographic response when these two forcings are allowed to interact. The weakened North America ridge in 2009/10 (known to be maintained by nonlinear interactions between heating and orography) can therefore possibly be explained by regions of weaker continental cooling over North America in 2009/10 compared to climatology (Figure 1.3a). Riviére and Drouard (2015) found that interaction between transient eddies and the background flow is particularly important in weakening the climatological Atlantic ridge in 2009/10, while contributing to the overall northeast weakening and southwest strengthening of the Atlantic ridge in 2013/14. Specifically, contrasting flow conditions in the North Pacific the two winters are thought to shape synoptic wave-trains favoring cyclonic/anticyclonic wave breaking, something which influences the NAO by shifting the Atlantic jet equatorward/poleward. In our study, the total effect of such eddy-mean flow interactions will be embedded partly in the transient response, partly in the nonlinear response. For 2013/14, the combined response to transients and stationary nonlinearity (Figure 4.5j) is in accordance with the results of Riviére and Drouard (2015), with a clear northeast weakening and southwest strengthening of the Atlantic ridge. For 2009/10, the weakening of the Atlantic ridge is mainly present in the nonlinear response (Figure 4.1e). This suggests that these eddy-mean flow

interactions, if as important as indicated by Riviére and Drouard (2015), were of a more nonlinear nature in 2009/10 compared to 2013/14.

5.3 Global warming

Both winter seasons investigated in this study occur during a time when accelerated warming of the climate system is present due to anthropogenic forcing. Global warming has the potential to affect the atmospheric circulation, but large natural variability operating on all time scales combined with a short observational record obscures potential systematic changes, and climate models are generally not robust in simulating these circulation-related aspects of climate change (Shepherd, 2014).

The role of global warming as an external forcing contributing to circulation anomalies such as those seen in 2009/10 and 2013/14 is not directly addressed in this study, but it is important to keep in mind that global warming modifies the atmospheric background state upon which the forcings are acting. This implies that the 2009/10 and 2013/14 background states could potentially favor a particular type of response as a consequence of ongoing global warming, compared to for instance a pre-industrial background state. As the global mean SST has increased since the beginning of the 20th century (Hartmann et al., 2013), it is also possible that the strength and/or frequency of the SST variability patterns we believe are important in 2009/10 and 2013/14 are altered due to global warming (Trenberth et al., 2015). Because the atmospheric circulation is so sensitive to the strength of the tropical forcing, a warmer background state combined with a warmer ocean surface in the equatorial region is perhaps the most obvious link between global warming and potential circulation changes. Other possibilities, such as the link between Arctic sea ice extent and midlatitude circulation discussed previously, are more tenuous due to large internal variability relative to the global warming signal.

5.4 Concluding remarks

The 2009/10 and 2013/14 winter circulation anomalies, and their driving mechanisms, have been investigated using a linear stationary wave model. As this

idealized model was shown to reproduce the observed circulation anomalies satisfactorily, it could be used to determine the isolated effect of orographic features, diabatic heating patterns, transient eddies, and nonlinear interactions in forcing anomalous circulation patterns the two winters, through a series of forcing experiments. The results from these forcing experiments have been analyzed, and physical driving mechanisms of the simulated forcing responses have been identified and discussed.

Anomalous heating is a dominant driver of the midlatitude circulation anomalies seen in 2009/10 and 2013/14, the most important part of which is believed to originate from warm tropical Pacific SST anomalies (El Niño event in 2009/10 and anomalously warm Pacific warm pool in 2013/14), in accordance with previous studies. Contrasting midlatitude circulation patterns were present during the two winters, with a weakened stationary wave pattern in 2009/10 and a strengthened stationary wave pattern over North America in 2013/14. These differences arise partly from differences in the diabatic heating response due to differences in the Pacific SST patterns, and partly from different eddy-mean flow interactions (where nonlinearity is important), expressed in the transient and the stationary nonlinear responses. In future studies a nonlinear stationary wave model could be used to explore these eddy-mean flow contributions further, while a comprehensive GCM could be used to capture the full effect of the tropical Pacific SST anomalies on the atmospheric circulation the two winters.

Bibliography

Alexander, M. A., Bhatt, U. S., Walsh, J. E., Timlin, M. S., Miller, J. S., and Scott, J. D. (2004). The atmospheric response to realistic arctic sea ice anomalies in an agcm during winter. *Journal of Climate*, 17(5):890–905.

Barnes, E. A. (2013). Revisiting the evidence linking arctic amplification to extreme weather in midlatitudes. *Geophysical Research Letters*, 40(17):4734–4739.

Barnes, E. A., Dunn-Sigouin, E., Masato, G., and Woollings, T. (2014). Exploring recent trends in northern hemisphere blocking. *Geophysical Research Letters*, 41(2):638–644.

Barnes, E. A. and Screen, J. A. (2015). The impact of arctic warming on the midlatitude jet-stream: Can it? has it? will it? *Wiley Interdisciplinary Reviews-Climate Change*, 6(3):277–286.

Brönnimann, S. (2007). Impact of el niño southern oscillation on european climate. *Reviews of Geophysics*, 45(2):n/a–n/a.

Chan, S. C. and Nigam, S. (2009). Residual diagnosis of diabatic heating from era-40 and ncep reanalyses: Intercomparisons with trmm. *Journal of Climate*, 22(2):414–428.

Chen, P. (2001). Thermally forced stationary waves in a quasigeostrophic system. *Journal of the Atmospheric Sciences*, 58(12):1585–1594.

Cohen, J., Screen, J. A., Furtado, J. C., Barlow, M., Whittleston, D., Coumou, D., Francis, J., Dethloff, K., Entekhabi, D., Overland, J., and Jones, J. (2014). Recent arctic amplification and extreme mid-latitude weather. *Nature Geoscience*, 7(9):627–637.

Deser, C., Tomas, R., Alexander, M., and Lawrence, D. (2010). The seasonal atmospheric response to projected arctic sea ice loss in the late twenty-first century. *Journal of Climate*, 23(2):333–351.

Francis, J. A. and Vavrus, S. J. (2012). Evidence linking arctic amplification to extreme weather in mid-latitudes. *Geophysical Research Letters*, 39(0):n/a–n/a.

Francis, J. A. and Vavrus, S. J. (2015). Evidence for a wavier jet stream in response to rapid arctic warming. *Environmental Research Letters*, 10(1):n/a–n/a.

Graf, H.-F. and Zanchettin, D. (2012). Central pacific el niño, the "subtropical bridge," and eurasian climate. *Journal of Geophysical Research: Atmospheres*, 117(D1):n/a–n/a.

Hartmann, D., Klein Tank, A., Rusticucci, M., Alexander, L., Brönnimann, S., Charabi, Y., Dentener, F., Dlugokencky, E., Easterling, D., Kaplan, A., Soden, B., Thorne, P., Wild, M., and Zhai, P. (2013). *Observations: Atmosphere and Surface. In: Climate Change 2013: The Physical Science Basis. Contribution of Working Group I to the Fifth Assessment Report of the Intergovernmental Panel on Climate Change*. Cambridge University Press, Cambridge, United Kingdom and New York, NY, USA.

Hartmann, D. L. (2015). Pacific sea surface temperature and the winter of 2014. *Geophysical Research Letters*, 42(6):1894–1902.

Held, I. M. and Ting, M. (1990). Orographic versus thermal forcing of stationary waves - the importance of the mean low-level wind. *Journal of the Atmospheric Sciences*, 47(4):495–500.

Held, I. M., Ting, M., and Wang, H. (2002). Northern winter stationary waves: theory and modeling. *Journal of Climate*, 15(16):2125–2144.

Honda, M., Inoue, J., and Yamane, S. (2009). Influence of low arctic sea-ice minima on anomalously cold eurasian winters. *Geophysical Research Letters*, 36(0):n/a–n/a.

Hoskins, B. J. and Karoly, D. J. (1981). The steady linear response of a spherical atmosphere to thermal and orographic forcing. *Journal of the Atmospheric Sciences*, 38(6):1179–1196.

Ineson, S. and Scaife, A. A. (2009). The role of the stratosphere in the european climate response to el niño. *Nature Geoscience*, 2(1):32–36.

Inoue, J., Hori, M. E., and Takaya, K. (2012). The role of barents sea ice in the wintertime cyclone track and emergence of a warm-arctic cold-siberian anomaly. *Journal of Climate*, 25(7):2561–2568.

Jaiser, R., Dethloff, K., Handorf, D., Rinke, A., and Cohen, J. (2012). Impact of sea ice cover changes on the northern hemisphere atmospheric winter circulation. *Tellus A*, 64(0):n/a–n/a.

Kalnay, E., Kanamitsu, M., Kistler, R., Collins, W., Deaven, D., Gandin, L., Iredell, M., Saha, S., White, G., Woollen, J., Zhu, Y., Chelliah, M., Ebisuzaki, W., Higgins, W., Janowiak, J., Mo, K. C., Ropelewski, C., Wang, J., Leetmaa, A., Reynolds, R., Jenne, R., and Joseph, D. (1996). The ncep/ncar 40-year reanalysis project. *Bulletin of the American Meteorological Society*, 77(3):437–471.

Kendon, M. and McCarthy, M. (2015). The uk's wet and stormy winter of 2013/2014. *Weather*, 70(2):40–47.

Kim, B. M., Son, S. W., Min, S. K., Jeong, J. H., Kim, S. J., Zhang, X. D., Shim, T., and Yoon, J. H. (2014). Weakening of the stratospheric polar vortex by arctic sea-ice loss. *Nature Communications*, 5(0):n/a–n/a.

King, M. P., Hell, M., and Keenlyside, N. (2015). Investigation of the atmospheric mechanisms related to the autumn sea ice and winter circulation link in the northern hemisphere. *Climate Dynamics*, 46(3-4):1185–1195.

Kushnir, Y., Robinson, W. A., Blade, I., Hall, N. M. J., Peng, S., and Sutton, R. (2002). Atmospheric gcm response to extratropical sst anomalies: Synthesis and evaluation. *Journal of Climate*, 15(16):2233–2256.

Palmer, T. (2014). Record-breaking winters and global climate change. *Science*, 344(6186):803–804.

Palmer, T. N. and Mansfield, D. A. (1984). Response of two atmopheric general circulation models to sea-surface temperature anomalies in the tropical east and west pacific. *Nature*, 310(9):483–485.

Perlwitz, J. and Graf, H. F. (1995). The statistical connection between tropospheric and stratospheric circulation of the northern-hemisphere in winter. *Journal of Climate*, 8(10):2281–2295.

Pithan, F. and Mauritsen, T. (2014). Arctic amplification dominated by temperature feedbacks in contemporary climate models. *Nature Geoscience*, 7(3):181–184.

Ringler, T. D. and Cook, K. H. (1997). Factors controlling nonlinearity in mechanically forced stationary waves over orography. *Journal of the Atmospheric Sciences*, 54(22):2612–2629.

Ringler, T. D. and Cook, K. H. (1999). Understanding the seasonality of orographically forced stationary waves: Interaction between mechanical and thermal forcing. *Journal of the Atmospheric Sciences*, 56(9):1154–1174.

Riviére, G. and Drouard, M. (2015). Understanding the contrasting north atlantic oscillation anomalies of the winters of 2010 and 2014. *Geophysical Research Letters*, 42(16):6868–6875.

Screen, J. A. and Simmonds, I. (2013). Exploring links between arctic amplification and mid-latitude weather. *Geophysical Research Letters*, 40(5):959–964.

Screen, J. A. and Simmonds, I. (2014). Amplified mid-latitude planetary waves favour particular regional weather extremes. *Nature Climate Change*, 4(8):704–709.

Seager, R., Kushnir, Y., Nakamura, J., Ting, M., and Naik, N. (2010). Northern hemisphere winter snow anomalies: Enso, nao and the winter of 2009/10. *Geophysical Research Letters*, 37(14):n/a–n/a.

Sellevold, R. (2015). *The linear stationary wave response to Arctic amplification related heating*. University of Bergen, Norway, (Unpublished Master's thesis).

Shepherd, T. G. (2014). Atmospheric circulation as a source of uncertainty in climate change projections. *Nature Geoscience*, 7(10):703–708.

Sobolowski, S., Gong, G., and Ting, M. F. (2011). Investigating the linear and nonlinear stationary wave response to anomalous north american snow cover. *Journal of the Atmospheric Sciences*, 68(4):904–917.

Ting, M. F. (1991). The stationary wave response to a midltatitude sst anomaly in an idealized gcm. *Journal of the Atmospheric Sciences*, 48(10):1249–1275.

Ting, M. F. (1994). Maintainance of northern summer stationary waves in a gcm. *Journal of the Atmospheric Sciences*, 51(22):3286–3308.

Ting, M. F. (1996). Steady linear response to tropical heating in barotropic and baroclinic models. *Journal of the Atmospheric Sciences*, 53(12):1698–1709.

Ting, M. F. and Held, I. M. (1990). The stationary wave response to a tropical sst anomaly in an idealized gcm. *Journal of the Atmospheric Sciences*, 47(21):2546–2566.

Ting, M. F., Wang, H. L., and Yu, L. H. (2001). Nonlinear stationary wave maintenance and seasonal cycle in the gfdl r30 gcm. *Journal of the Atmospheric Sciences*, 58(16):2331–2354.

Trenberth, K. E., Fasullo, J. T., and Shepherd, T. G. (2015). Attribution of climate extreme events. *Nature Climate Change*, 5(8):725–730.

Wallace, J. M., Held, I. M., Thompson, D. W. J., Trenberth, K. E., and Walsh, J. E. a. (2014). Global warming and winter weather. *Science*, 343(6168):729–730.

Wang, H. and Ting, M. (1999). Seasonal cycle of the climatological stationary waves in the ncep-ncar reanalysis. *Journal of atmospheric sciences*, 56(22):3892–3919.

Wang, S. Y., Hipps, L., Gillies, R. R., and Yoon, J. H. (2014). Probable causes of the abnormal ridge accompanying the 2013-2014 california drought: Enso precursor and anthropogenic warming footprint. *Geophysical Research Letters*, 41(9):3220–3226.